CHAPTER 11

Advances in X-ray crystallography methods to study structural dynamics of macromolecules

Ali A. Kermani[a,*], Swati Aggarwal[b], and Alireza Ghanbarpour[c]
[a]Department of Molecular, Cellular, and Developmental Biology, University of Michigan, Ann Arbor, MI, United States
[b]BioMAX, MAXIV Laboratory, Lund, Sweden
[c]Department of Biology, Massachusetts Institute of Technology, Cambridge, MA, United States

1. Introduction

X-ray crystallography has been one of the greatest scientific tools developed in the 20th century. This technique has enabled molecular biologists to understand and explain some of the most critical fundamental processes of biological systems. Structure determination of proteins using X-ray crystallography was initiated when John Kendrew and Max Perutz unraveled the structure of myoglobin [1] and hemoglobin [2], respectively, in the late 1950s. Other significant milestones in the field of protein X-ray crystallography are the structure elucidation of nucleic acid-protein complexes by Aaron Klug [3]; the structure of the photosynthetic reaction center by Johann Deisenhofer, Hartmut Michel, and Robert Huber [4]; the structure of F1 ATPase by John Walker [5]; the structure of potassium channels by Roderick Mackinnon [6]; the structure of RNA polymerase by Roger Kornberg [7]; and the first structure of G-protein coupled receptor (GPCR) by Brian Kobilka [8].

According to the Protein Data Bank (PDB) statistics, X-ray crystallography (with over 167,000 entries as of July 2022) is the primary technique for structure determination of both cytosolic and membrane proteins (https://www.rcsb.org/stats/growth/growth-xray). Membrane proteins account for 20%–30% of the proteome in most organisms [9] and play critical roles in a wide range of biological processes such as signal transduction, respiration, molecular transport, and cell-cell communication in eukaryotes

* Current address: Department of Structural Biology, St. Jude Children's Research Hospital, Memphis, TN, United States.

Advanced Spectroscopic Methods to Study Biomolecular Structure and Dynamics
https://doi.org/10.1016/B978-0-323-99127-8.00020-9

and conferring multidrug resistance in pathogenic bacteria. Membrane proteins, mainly GPCRs, ion channels, and receptor tyrosine kinases, are the target of more than 60% of the current drugs on the market [10,11]. The structural information of membrane proteins has facilitated our understanding of the molecular details of signal transduction [12–15] and selective ion conduction [16,17] across the cell membrane and to design novel structure-based drugs [18].

However, elucidating the structure of proteins using X-ray crystallography is associated with multiple obstacles that impede the rate of solving new crystal structures. Some of these challenges include difficulty in obtaining large amounts of the target protein; extracting and solubilizing membrane proteins; stabilizing purified proteins; generating single, large, and well-diffracting crystals; phasing novel protein structures; and finally dealing with crystallographic defects such as high levels of anisotropy and mosaicity [19]. Recent technological advances have aided crystallographers in overcoming some of these challenges [20,21]. Advances in sample preparation, automation, and computational programs minimize the sample volume, lower the cost, and accelerate the process of generating crystals, screening crystals, data collection, and data processing. They enable high-throughput crystal screening, processing data collected from twinned or multicrystal samples, and generating single crystals from liquids by applying pressure [22]. In this chapter, we summarize some of the recent developments in the field of protein X-ray crystallography that have enabled the high-resolution structure determination of challenging proteins, particularly membrane proteins. These include (i) novel detergents and solubilization reagents, (ii) strategies to improve stabilization and increase crystallization likelihood, (iii) methods to assess the homogeneity and purity of protein samples, (iv) new crystallization methods, (v) new crystallization additives, and (vi) advances in instrument and data-processing software.

2. Protein extraction and purification

The first bottleneck in macromolecular X-ray crystallography is to generate sufficient amounts of target protein in stable, monodispersed, and aggregation-free states [23]. This can be achieved by optimizations and strategical modulations of several conditions [20].

2.1 Detergents and surfactants

Compared to soluble proteins, membrane proteins mostly express in low quantities and are more prone to denaturation and aggregation [19]. This is because membrane proteins are embedded in the phospholipid bilayer,

and thus, their extraction requires utilizing amphiphilic molecules, such as detergents. The amphiphilic detergents with a hydrophobic tail and a hydrophilic head group enable them to solubilize membrane proteins by enclosing the hydrophobic core of membrane proteins, whereas the loops and hydrophilic regions remain exposed to the aqueous environment [19]. However, breaking lipid-protein and protein-protein interactions during the solubilization process can adversely affect the stability and function of membrane proteins. Here, we introduce some of the most recently developed detergents with enhanced features to improve the solubilization and stabilization process of membrane proteins. These advances in extraction and solubilizing methods have accelerated the production of eukaryotic membrane proteins for X-ray structural studies.

2.1.1 Maltose-neopentyl glycol (MNG) compounds

Maltose-neopentyl glycol (MNG) compounds were introduced in 2010 as a new class of amphiphiles suitable for direct extraction and solubilization of membrane proteins from lipid bilayers (Table 1) [24]. MNG has facilitated the purification and structure determination of several challenging membrane proteins, including GPCRs and ABC transporters (Table 2). The high efficacy of MNG in extracting and solubilizing membrane proteins is attributed to its ability to pack compactly during the micelle formation process

Table 1 The most recently developed detergents for use in membrane protein crystallography.

Detergent	Detergent type	Chain length	CMC (%, mM)	Reference
Decyl maltose neopentyl glycol (DMNG)	Nonionic	10C	0.036 mM 0.0034%	[24]
Undecyl maltose neopentyl glycol (UMNG)	Nonionic	11C	–	Anatrace website
Lauryl maltose neopentyl glycol (LMNG)	Nonionic	12C	0.01 mM 0.001%	[24]
Octyl glucose neopentyl glycol (OGNG)	Nonionic	8C	1.02 mM 0.058%	[26]
NAPol	Nonionic	–	2%	[27]
Calixarene	Anionic	3C to 12C	0.05 to 1.5 mM	[28]
Fluorinated octyl maltoside	Nonionic	6F	0.7 mM	[29]

Table 2 List of some membrane protein structures solved using novel detergents, see text.

Detergent	Membrane protein	PDB code	Resolution (Å)	Reference
Maltose-neopentyl glycol (MNG)	β_2 adrenrgic receptor (β_2AR)	3SN6	3.2	[15]
LMNG	Agonist-β_2 adrenoceptor complex	3PDS	3.5	[30]
LMNG	M3 muscarinic acetylcholine receptor	4DAJ	3.4	[31]
LMNG	Neurotensin receptor NTS1	4GRV	2.8	[32]
LMNG	TatC	4B4A	3.5	[33]
LMNG	TRPA1 ion channel	3J9P	4.24	[34]
LMNG	OX2 orexin receptor bound to the insomnia drug suvorexant	4S0V	2.5	[35]
LMNG	Rhodopsin-Arrestin complex	4ZWJ	3.3	[36]
LMNG	ABC transporter PglK	5C78	2.9	[37]
LMNG	MFS transporter Ferroportin	5AYN	2.2	[38]
LMNG	TRPA1 ion channel	3J9P	4.24	[34]
LMNG	Influenza hemagglutinin	6HJN	3.3	[39]
LMNG	Rhodopsin-transducin	6OYA	3.3	[40]
LMNG/CHS mixture (8:1)	DUOX1-DUOXA1	6WXR 6WXU	3.2	[41]
LMNG/CHS mixture (8:1)	KCNQ1 potassium channel	6UZZ 6V00	3.1	[42]
DMNG	TRPV2 ion channel	5HI9	4.4	[43]
DMNG	H^+/Ca^{2+} exchanger	4KPP	2.3	[44]
OGNG/CHS	K^+ channel TREK-2	4BW5	3.2	[45]
NAPol	TOM core complex	5O8O	6.8	[46]
NAPol	Photosystem I supercomplex	Cryo-EM	6.9	[47]
NAPol	Photosystem II supercomplex	Cryo-EM	5.8	[48]
Calixarene	Potassium chloride cotransporter KCC2	Cryo-EM	15	[49]

(Table 1). This results in an exceptionally low critical micelle concentration (CMC) (as low as 11 nM) [25], improvement of protein stability (indicated by an increase in thermal stability of MNG-solubilized proteins), and an increase in water solubility of MNG micelles. Fig. 1A illustrates the structure

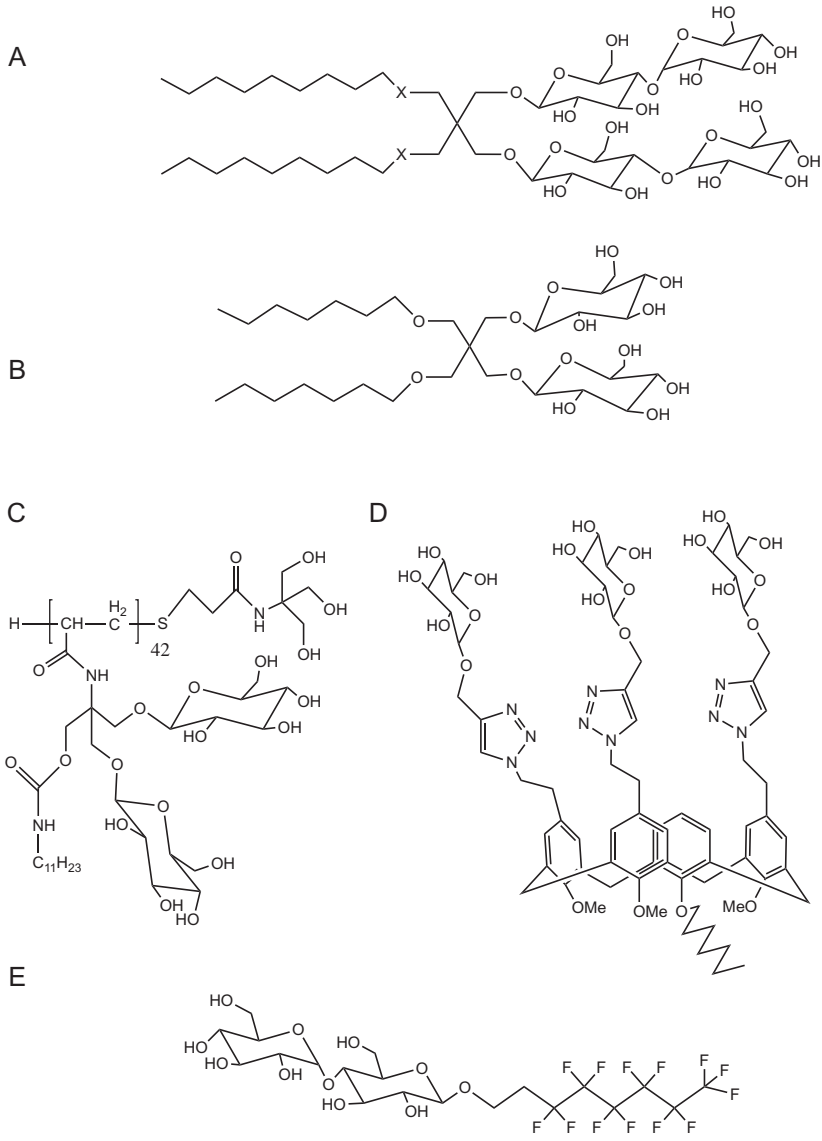

Fig. 1 Chemical structures of some of the novel detergents developed for membrane proteins' purification and stabilization: (A) maltose neopentyl glycol (MNG), (B) glucose neopentyl glycol (GNG), (C) NAPol, (D) calixarene, and (E) fluorinated octyl maltoside.

of a representative MNG in which two hydrophilic heads, each made of a maltose unit, are connected to two *n*-decyl lipophilic chains via a quaternary carbon and variously an amide, ether, or aliphatic moiety [24]. In order to crystallize membrane proteins with different numbers of transmembranes (TMs) and intracellular and extracellular loop sizes, MNG amphiphiles with varying chain lengths have been generated. Lauryl maltose neopentyl glycol (LMNG), with 12 carbon chain lengths and more than 10 published structures, is the most successful member of the MNG class in determining the crystal structure of membrane proteins (Table 2). Decyl maltose neopentyl glycol (DMNG) (10 carbon chain length) occupies the second place in this class with two solved crystal structures (Table 2). Undecyl maltose neopentyl glycol (UMNG) is the most recent member of this class, which carries a chain composed of 11 carbons. UMNG was created recently to provide an intermediate chain length between LMNG and DMNG.

2.1.2 Glucose-neopentyl glycerol (GNG) compounds

The next class of detergents, glucose-neopentyl glycerols (GNGs), is developed based on MNG detergents, in which the maltose moiety is replaced with glucose (Fig. 1B) [26]. As a result, GNG amphiphiles form smaller micelles compared to their MNG counterparts and provide an extra hydrophilic surface area necessary to form crystal contacts (Table 1). However, lower efficacy in stabilizing membrane proteins, compared to the MNG class [26], is the main drawback of GNG and explains the limited number of solved protein structures in the presence of this detergent (Table 2). One possible strategy to exploit the benefits of both classes (MNG is more efficient in stabilizing membrane proteins, whereas GNG promotes crystallization by providing a larger surface area) is to extract and solubilize the target protein using the MNG class and transfer the MNG-solubilized protein into the GNG detergent immediately before setting up the crystal trays, for instance, during size exclusion chromatography (SEC).

2.1.3 Nonionic amphipols (NAPol)

It is crucial to retain membrane proteins extracted from lipid bilayers in a functional form throughout the purification process when the molecular mechanism of the target protein needs to be elucidated using X-ray crystallography. However, detergents can impact the activity of solubilized membrane proteins by forming protein-free micelles in the solution [50]. Free micelles can affect the stability of extracted proteins by disrupting protein-protein interactions and thus influencing the structural determination

efforts by phase separation during crystallization. Nonionic amphipols (NAPoI) are a new class of amphipols that stabilizes membrane proteins in the aqueous solution by forming small globular particles made of two glucose molecules and one undecyl chain with a diameter of about 6 nm [27] (Fig. 1C). The amphipathic nature of amphipols enables them to stabilize membrane proteins while preserving the native state of membrane proteins, demonstrating a gentler alternative to detergents. Membrane proteins are usually transferred to NAPol after initial extraction and solubilization using conventional detergents. In a study elucidating the function of GPCRs, Granier's lab demonstrated that GPCRs reconstituted in NAPols are highly functional and show the same activity as in living cells [51]. Similarly, NAPol proved to be essential for determining the structure of the TOM complex, the central entry gate for precursor proteins into mitochondria [46]. NAPol has proved to be highly beneficial in stabilizing protein complexes and solving their structures using cryo-electron microscopy (cryo-EM) [47,48].

2.1.4 Calixarene

Calixarene is a new class of detergents based on the calix[4]arene scaffold, in which three negatively charged methylene-carboxylate groups are attached to one side of the scaffold, and the other side harbors a single hydrophobic chain, 1–12 carbon chain long (Fig. 1D) [28]. Depending on the length of the hydrophobic tail, the CMCs of these detergents vary from 1.5 mM (3C) to 0.05 mM (12C). Similar to other detergents, calixarene maintains the membrane proteins in solution by forming micellar structures; however, in some cases, it further improves the stability of purified membrane proteins by establishing a series of salt bridges with positively charged residues located on the intracellular loops of these proteins [28]. Potassium chloride cotransporter KCC2 [49] and influenza viral envelope matrix protein 2 (M2) [52] are a few examples that were successfully purified and solubilized in the functional form using this new class of detergents.

2.1.5 Fluorinated surfactants

Fluorinated surfactants are another class of surfactants specifically designed to improve the stability of extracted membrane proteins rather than de novo solubilizing membrane proteins from lipid bilayers. Fluorinated surfactants possess a similar structure to classical detergents, except that they carry a segment of fluorine in their hydrophobic tails (Fig. 1E) [29,53]. The fluorinated chain makes the hydrophobic tail lipophobic and therefore impermeable to

the lipid bilayer and unable to solubilize membrane proteins [53]. As a result, fluorinated surfactants are not very common among membrane protein biochemists and are considered nonconventional surfactants. However, given that fluorinated surfactants are less efficient than detergents in breaking protein-protein and protein-lipid interactions, they are more capable of maintaining the essential lipids bound to the membrane proteins and, therefore, more likely to maintain the solubility and activity of purified membrane proteins, as has been shown for bacteriorhodopsin and cytochrome b_6f complex [54] and ryanodine receptor [55].

2.1.6 Commercial detergent screen kits

Identifying the most stabilizing detergents for solubilization and crystallization purposes can be laborious, time-consuming, and costly. Therefore, to facilitate this process, commercial detergent screens have been developed. Hampton Research Detergent Screen is a Deep Well block composed of 96 mild detergent reagents ready to use in solubilization or crystallization efforts (https://hamptonresearch.com/product-Detergent-Screen-723.html). These detergents represent some of the most promising classes of detergents extracted from the literature and past membrane protein work. They can be supplemented into the protein solution to explore the impact of individual detergents on the solubility of protein of interest during the purification process or used as an additive just before setting up crystal trays. Using these commercially available detergent screens, we have identified some detergents vital for obtaining the first high-resolution crystal structures of the small multidrug resistance (SMR) transporters [56,57].

2.2 Membrane mimetics

As discussed earlier, detergents can have deleterious effects on the stability and activity of solubilized membrane proteins. Therefore, detergent alternatives have gained significant attention during the past 2 decades. Membrane mimicking systems, such as nanodiscs, styrene-maleic acid copolymer lipid particles (SMALPs), and the saposin-lipoprotein nanoparticle system (Salipro), have been developed to minimize or eliminate the need to use detergents for purification and solubilization purposes and, therefore, to better preserve the integrity and function of target membrane proteins. Numerous reports currently demonstrate the success of membrane mimicking systems in structural and functional studies of membrane proteins using nuclear magnetic resonance (NMR), cryo-EM, surface plasmon resonance (SPR), small-angle X-ray scattering (SAXS), and X-ray crystallography [58,59].

2.2.1 Nanodiscs

One of these artificial lipid environments that have proved to be an efficient tool in structural and functional studies of membrane proteins is the nanodisc. Nanodiscs are discoidal patches of lipid bilayers surrounded by two molecules of amphipathic (having both hydrophilic and hydrophobic regions) helical scaffold proteins, the so-called MSP [60]. Nanodiscs provide a more native-like environment, which can improve the stability and function of the reconstituted protein [61]. Nanodisc assembly occurs instinctively when detergent-solubilized membrane protein is mixed with lipid bilayers and MSP scaffold protein, and the solubilizing detergent is gradually removed during dialysis or using biobeads [62,63]. The ratio between lipids, MSP, and membrane protein is determined empirically and is highly important for monodisperse and functional nanodisc formation.

Nanodiscs have gained more momentum in the lipidic cubic phase (LCP) and cryo-EM than in X-ray crystallography. The first solved structure of a membrane protein embedded into a nanodisc was the TM protein bacteriorhodopsin [58]. Bacteriorhodopsin was first solubilized using *n*-dodecyl-β-D-maltoside (DDM) and then reconstituted into MSP1 and MSP1E3D1 (a variant of MSP1 that contains three additional helices and is suitable for generating larger nanodiscs) nanodiscs and employed for crystallization. Surprisingly, traditional crystallography did not generate any crystals from bacteriorhodopsin-embedded nanodiscs unless an LCP monoolein (1-oleoyl-rac-glycerol) environment was used; this maneuver yielded high-resolution (1.8–2.0 Å) diffracting crystals [58]. Another example is the cryo-EM structure of a multidrug-resistant efflux protein AdeB from *Acinetobacter baumannii* [64]. Similar to bacteriorhodopsin, AdeB was initially solubilized in DDM and subsequently reconstituted into MSP1E3D1 nanodiscs. The structure was solved to 2.98 Å resolution and unraveled the binding site for several drugs as substrates for this transporter [64].

2.2.2 Styrene maleic acid copolymer lipid particles (SMALPs)

We discussed the importance of nanodiscs in structural studies of membrane proteins; however, the main drawback of using nanodiscs is their inefficacy in extracting membrane proteins from lipid bilayers. Therefore, the need to use traditional methods using detergents for the initial stages of extraction and solubilization remains in place [59,65]. To overcome this issue, detergent-free approaches have been developed. SMALPs are synthetic polymers composed of styrene (hydrophobic) and maleic acid (hydrophilic). The amphipathic features of SMALPs enable them to solubilize membrane

proteins by encapsulating them with a patch of the surrounding lipid bilayer. The use of this platform can significantly affect the stability and functionality of solubilized membrane proteins because some of the associated lipids essential for the activity of these proteins remain bound throughout the purification process [66,67]. One of the early works on structural studies of membrane proteins using SMALP was performed on *Escherichia coli* secondary transporter AcrB [65]. AcrB was extracted and solubilized using SMALP, negative-stained, and visualized under an electron microscope. Although a low-resolution (>15 Å) structure was obtained, the entire solubilization and data collection were carried out in less than 1 week, which was significantly faster than that of similar structures obtained using X-ray crystallography at that time. In a recent work, the structure of the same protein, AcrB, was determined at 3.2 Å resolution using cryo-EM [68]. This new structure revealed the presence of patches of the lipid bilayer within the AcrB TM domain, likely essential for the function of this multidrug transporter. The crystal structure of AcrB extracted in the presence of detergents was devoid of these lipid patches, demonstrating the importance of detergent-free systems in preserving the native structure of proteins [68].

2.2.3 Saposin-lipoprotein nanoparticle system (Salipro)

A more recently developed artificial membrane-like environment for structural and functional studies of membrane proteins is the saposin-lipoprotein nanoparticle system, Salipro [69]. Salipro is comparable to nanodiscs in several different aspects. Salipro, similar to nanodiscs, is composed of lipid patches surrounded by a scaffold protein, which in this case is saposin A instead of apolipoprotein A-1. Saposin A is a known lipid membrane modulator with lipid-binding characteristics [69]. The presence of six invariable cysteine residues that make disulfide bridges in the structure of saposin A makes it an unusually stable protein [70]. The self-assembly of Salipro discs occurs when the detergent-solubilized membrane protein is combined with lipids and saposin A in an empirically determined ratio, and the detergent is removed over a relatively short period of time. The number of saposin A molecules that encapsulate the lipid core can vary based on the size of the membrane protein. This enables saposin A to be highly flexible and form stable and homogeneous Salipro discs based on the size of the incorporated membrane protein [69]. This property of Salipro nanoparticles presents a significant advantage over nanodiscs, which have a fixed diameter based on the length of the scaffolding apolipoprotein belt. The membrane protein incorporated into Salipro disc nanoparticles maintains

its solubility, monodispersity, and oligomeric state and remains stable over a wide range of temperatures (0–95°C) [69]. Although Salipro, similar to nanodiscs and SMALPs, is mainly designed for the structural determination of membrane proteins using Cryo-EM, it can also be used for the biochemical and biophysical characterization of these macromolecules an the aqueous solution, providing complementary tools for structural studies using X-ray crystallography.

3. Increasing the solubility and stability of proteins

3.1 Crystallization chaperones

Generating diffraction-quality crystals remains a major challenge in obtaining high-resolution structural information on target proteins. Incorporating fusion partners into the target protein has proved to be an efficient tool for improving the solubility and stability of proteins and therefore increasing the crystallization likelihood. One of the earliest fusion proteins employed for this purpose is the maltose-binding protein (MBP) [71]. The PDB database shows that MBP is the most successful fusion protein for crystallizing soluble proteins. MBP is the periplasmic portion of the ATP-binding cassette (ABC) maltose/maltodextrin transporter. The MBP tag is mostly cleaved through specific proteolytic sites engineered in the linker region between the tag and the protein of interest. However, during tag removal, several difficulties might originate, such as a decrease in the yield of the target protein, precipitation of the target protein, or production of an inactive protein. One possible solution to these problems is to retain the tag during the crystallization process. Nonetheless, multidomain proteins are typically less prone to form well-ordered, diffracting crystals, perhaps because of conformational heterogeneity originated by flexible linker regions [72]. Recently, it has been shown that generating a rigid construct with an MBP tag is a promising strategy for crystallizing alpha-helical proteins [73]. In this approach, MBP is added to the N-terminus of the target protein in such a way that the last helix of MBP and the first helix of the target protein form a continuous helix (Fig. 2A). This approach has been more successful by adding alanine linkers, which induce alpha-helical propensity between MBP and the target protein. MBP fusion protein structures deposited in PDB depict that although most of these structures comprise short interdomain linkers, some are crystallized using long linkers. In several other cases, a mutated version of MBP has been shown to facilitate crystal formation by lowering the surface entropy. Furthermore, overlapping the fused and unfused structures demonstrates that

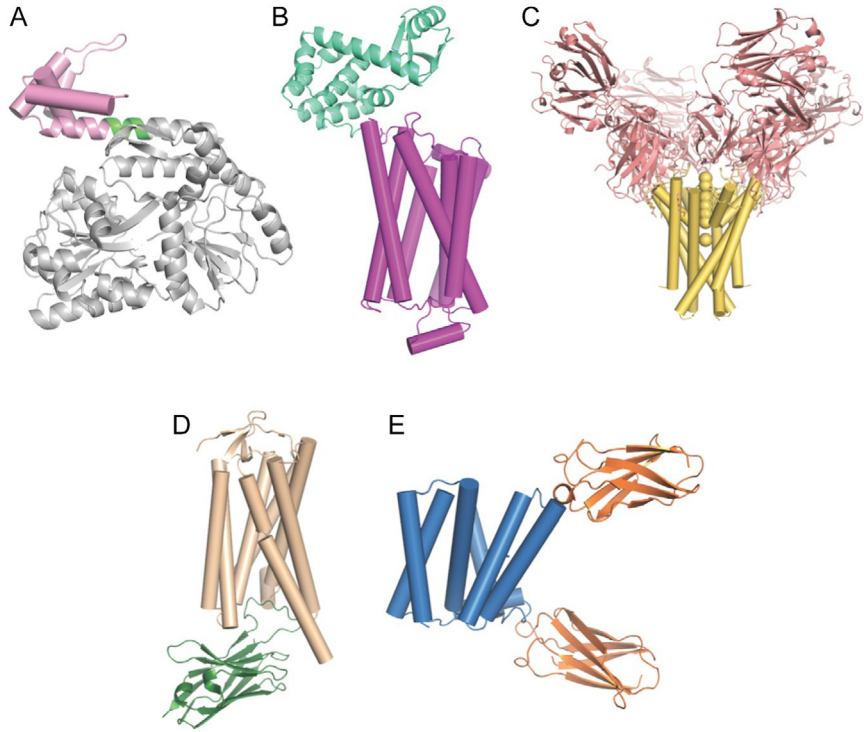

Fig. 2 Crystallization chaperones developed for structural and functional studies of proteins: (A) crystal structure of hNLRP12-PYD (pink) bound to maltose-binding protein (gray) (PDB code 5H7N). The linker between the two fusion partners is shown in green. (B) Crystal structure of the human β2-adrenergic G protein-coupled receptor (purple) bound to T4 lysozyme (green cyan) (PDB code 2RH1). (C) Crystal structure of potassium channel KcsA (yellow) solved in the presence of Fab (pink) (PDB code 1K4C). (D) Crystal structure of angiotensin II type 1 receptor (wheat) stabilized using nanobody S1I8 (dark green) (PDB code 6DO1). (E) Crystal structure of the Gdx-Clo (dark blue) in the presence of the monobody (orange) (PDB code 6WK8). Protein macromolecules are shown in cylindrical shapes to make an easier distinction between the proteins and crystallization chaperones.

MBP does not contribute to the structural modifications of the target protein. Additionally, a mammalianized version of MBP (mMBP) was recently employed to produce highly posttranslationally modified eukaryotic proteins that are transiently expressed in mammalian cells. mMBP harbors mutations that improve both MBP solubility and affinity purification as well as enhance the crystallizability of MBP fusion proteins [74].

In the case of membrane proteins, crystallization chaperones have proved to be exceedingly efficient in i) improving the stability of membrane

proteins and ii) expanding the crystallization surface area and subsequently enhancing the likelihood of crystallizing these proteins [75,76]. Membrane proteins are inherently dynamic, which enables them to fulfill their biological roles [77]. This flexibility, however, can increase conformational heterogeneity and prevent crystal contact formation. Even formed crystals might represent crystallography defects or diffract poorly. Crystallography chaperones can overcome this obstacle by locking the target protein into a fixed conformation, lowering conformational entropy and hence triggering uniform packing. In addition, crystallization chaperones further promote crystallization by masking highly unstable or flexible protein regions [75]. More importantly, chaperone fused to the membrane protein expands the hydrophilic surface area necessary for crystal contact formation. Membrane proteins are mainly composed of hydrophobic residues embedded in the lipid bilayer or detergent micelles upon solubilization, with a few hydrophilic loops present in the solvent, accessible for crystal contact formation. The small hydrophilic surface area available for crystal contact formation is one of the main reasons for the low crystallization rate of membrane proteins.

One of the successful examples of crystallography chaperones is T4 lysozyme. The application of T4 lysozyme as a crystallography chaperone is based on the idea that fusing an easy crystallizing partner to the target protein can facilitate the crystallization of the target protein. T4 lysozyme has been successfully used to solve the crystal structure of several GPCRs, including β_2-adrenergic receptor (β_2AR) [78], CXCR4 chemokine receptor [79], histamine H1 receptor [80], and dopamine D3 receptor [81]. In all these cases, T4 lysozyme was covalently linked to the protein by replacing an entire cytoplasmic loop (Fig. 2B). Although this strategy was crucial for the structure determination of these membrane proteins, in some cases, it impeded the functionality of the protein [82], raising the concern that introducing these changes might negatively impact the protein structure. In addition, the process of constructing T4 lysozyme fusion can be costly and laborious because the placement of T4 lysozyme on the target protein is important for a protein's solubility and functionality. This can only be determined empirically by generating numerous constructs and investigating the overexpression and thermal stability of each recombinant protein separately. Thus, the popularity of T4 lysozyme as a crystallization chaperone has drastically declined over the past decade.

Monoclonal antibodies specific to the target membrane protein have also been used as crystallization chaperones. Compared to the traditional

antibody generation process in which antibodies are directly collected from plasma upon immunization, in the case of monoclonal antibodies, cells that produce antibodies and lymphocytes are harvested from the spleen or lymph nodes. They have an extended life expectancy through fusion with cancerous B-cells or myelomas. In this way, the resulting hybridoma cells are immortal and able to produce large amounts of monoclonal antibodies for many generations. Purified monoclonal antibodies are subjected to proteolysis to remove the fragment crystallizable region (Fc) and retain the antigen-binding fragment (Fab). Monoclonal antibodies can recognize a specific epitope on the target protein with extremely high affinity in the range of 20–200 pM (with an average of 66 pM) [83]. Using this rigorous process, monoclonal antibodies were efficient for stabilizing and solving the crystal structures of numerous proteins, including cytochrome *c* oxidase from *Paracoccus denitrificans* [84], K^+ channel KcsA [85], the ClC chloride channel [86], nitric oxide reductase [87], the SecYE protein-conducting channel [88], and so on (Fig. 2C). However, raising monoclonal antibodies specific to the understudy membrane protein can be time-consuming and expensive and may not be successful for every membrane protein.

A nanobody is an alternative crystallization chaperone to antibodies, which has proved to be beneficial in crystallizing membrane proteins, particularly GPCRs [89]. Nanobodies are single variable domains of camelid antibodies, which form the entire antigen-binding surface (Fig. 2D). Compared to conventional antibodies that are composed of two heavy chains and two light chains with both heavy and light chains contributing to form the antigen-binding surface, camelid antibodies are composed only of heavy chains forming a unique variable fragment, termed VHH or Nb. Nanobodies are composed of nine antiparallel β-strands connected by short loops (Fig. 2D). The antigen-binding interface of the nanobody consists of three loops designated as complementarity determining regions (CDRs). Out of these three loops, CDR3, which is the longest loop and plays the most critical role in antigen recognition, has been the subject of most randomization [90]. Randomization of CDRs enables nanobodies to conform to the epitope site on the surface of the target protein. Several different nanobody libraries have been developed to facilitate the screening and increase the number of binders. While previous generations of nanobodies were raised by immunization of camelids [91], new platforms are based on a fully synthetic library displayed on the yeast surface [90,92] or ribosome display [93]. The use of a fully synthetic library not only lowers the cost of nanobody

generation and saves time substantially but also, importantly, addresses the immunological tolerance to self-antigens in the host [90]. Many of the medically important targets represent a high sequence similarity with their camel homologs; therefore, because of immunity to self-antigens, generating efficient antibodies is very challenging and, in many cases, impossible [94].

Enriching the target protein against the naïve library is performed during two rounds of magnetically activated cell sorting (MACS). MACS is a low-cost, highly efficient cell separation technique based on cell surface antigens. During each round of enrichment, the target protein is labeled with a distinct fluorophore, exposed to the nanobody expressing yeast library, followed by removing the excess of the target protein. High-affinity binders are isolated using antifluorophore magnetic microbeads. Before each selection round, it is crucial to ensure depleting the library from nonspecific nanobodies, which might bind to reagents, such as magnetic beads or fluorescent tags. The two commonly used fluorescent tags are Alexa Fluor 647 and fluorescein isothiocyanate (FITC). Using a distinct tag during each round of selection prevents enriching the fluorescent tags [90]. In the end, active clones are separated by fluorescence-activated cell sorting (FACS), which involves expressing the enriched library, staining with fluorescent-tagged protein, and sorting the cells based on the fluorescence of the tag attached to the antigen. The nanobody platform has aided the structure determination of several membrane proteins, including angiotensin II (AngII) type 1 receptor (AT1R) [94], KDEL receptor from Golgi [95], ABC exporter TM287/288 [96], mycobacterial ABC exporter IrtAB [97], and SARS-CoV-2 receptor-binding domain [98].

Monobodies present another distinct class of crystallization chaperones. They are synthetic binding proteins based on the human fibronectin type III domain (FN3), composed of a scaffold of seven antiparallel β-strands connected by three loops on each side of the protein (Fig. 2E) [99]. The general architecture of this scaffold is conserved among monobodies; however, the loops [99,100] or a combination of loops and β-sheets [101] are diversified to create new binders. Monobodies resemble antibodies by creating a binding surface for other proteins; however, they offer unique advantages over antibodies. Monobodies are small, monomeric proteins with about 100 residues and ∼10 kDa, whereas antibodies are much larger, usually ∼50 kDa. The small size of monobodies makes them ideal crystallization chaperones for small membrane proteins and structural studies of membrane proteins by NMR. An excellent example of small membrane proteins is the SMR family that formed high-resolution diffracting crystals only in the presence of a

monobody (Fig. 2E) [56,102]. Furthermore, compared to antibodies, which require an oxidizing environment to form disulfide bonds and retain activity, monobodies do not form disulfide bonds and therefore can remain active under reducing conditions. This makes overexpression of monobodies in *E. coli* a feasible task [99]. Monobodies have played a significant role in expanding our understanding of the molecular mechanism of membrane proteins, particularly the mechanisms that regulate molecular recognition [103]. Monobodies tend to mimic the natural ligands and bind to the functional site on the target protein. The flexibility of the loops on the monobody scaffold enables them to enter and occupy the binding site, thereby providing a platform to compare the properties of the functional site in the presence of the natural ligand versus monobody [103]. In this regard, the crystal structure of two bacterial homologs of a dual topology fluoride ion channel (Fluc) was solved in the presence of three different monobodies [104]. The presence of monobodies was crucial for obtaining high-resolution diffracting crystals to unveil the unique two-pore architecture of these proteins while providing clear evidence of the dual-topology conformation within members of the Fluc family [104].

The selection process for high-affinity binders involves several rounds of sorting in which the biotinylated target protein is exposed to the phage display library carrying $\sim 2 \times 10^9$ clones. The target protein bound to its high-affinity binder is captured using streptavidin-coated magnetic beads, and nonspecific clones are washed away. The target protein bound to the monobody is released from the beads by cleaving the biotinylation linker using dithiothreitol or other reducing agents [105]. The recovered phage particles are amplified by infecting *E. coli* cells and using them during the next round of sorting. The desired phage clones with the highest affinities are sequenced and cloned in expression vectors for overexpression and purification.

In all these platforms, fusing a second soluble protein, which specifically binds the target membrane protein, crystallization chaperone, is the main key for expanding the surface area required to form crystal contacts, masking the disordered regions and subsequently increasing the likelihood of crystallizing the TM region. Similarly, one can use other intrinsic domains surrounding the TM region, mainly soluble domains such as cytoplasmic and extracellular domains, as pseudocrystallization chaperones to facilitate the crystallization of this region of the membrane protein of interest. Solving the crystal structure of the membrane-embedded domain of histidine kinase NarQ provides an interesting example of the efficacy of a pseudocrystallization chaperone. NarQ is a nitrate/nitrite sensor kinase composed of seven

domains: the periplasmic sensor domain, TM domain, HAMP domain, signaling helix, GAF-like domain, DHp domain, and kinase CA domain [106]. In the absence of sensor and HAMP domains, the TM domain crystallized after 3 months and diffracted to 2.3 Å resolution [107]. It was observed from the structure that residues adjacent to the truncation site are largely disordered. Strikingly, the full-length protein composed of sensor-TM-HAMP crystallized faster, under 2 weeks, and diffracted to a higher resolution of 1.9 Å with well-ordered TM helices and loops [106]. Although the binding site in both proteins was fully ordered, the full-length structure was more beneficial in understanding the signaling process.

3.2 Thermostabilizing mutations

An alternative strategy to crystallization chaperones is the systematic mutagenesis of proteins to make them thermostable and, therefore, more amenable to crystallization [108]. There are numerous examples of stabilizing and crystallizing soluble proteins using this technique [109–113]. In this technique, known as surface entropy reduction (SER), multiple residues on the protein's surface are engineered to lower the conformational entropy and increase its propensity to crystallization [114]. The SERp server (http://services.mbi.ucla.edu/SER/) has been designed to identify such residues [115]. Compared to soluble proteins, membrane proteins are inherently more flexible and unstable, and generating diffracting crystals of these proteins poses a greater challenge. Therefore, generating the thermostable versions of these proteins appears to be essential for efficient crystallization.

Introducing a single-point mutation or a combination of single-point mutations in the structure of membrane proteins can cause an increase in the membrane protein rigidity, a decrease in conformational exchange, a reduction in site-specific tensions, and an increase in the number of ordered water molecules and therefore can result in an improvement in the thermostability of membrane proteins and subsequently an increase in the crystallization probability of target protein [116]. One of the main advantages of this strategy over the crystallization chaperones is the tendency of thermostabilized proteins to crystallize with different ligands. For example, the cocrystal structure of thermostabilized b1-adrenergic receptor (b1AR) with 12 different ligands has been solved, facilitating the detailed understanding of ligand binding and receptor activation [117–120]. On the other hand, the laborious and high cost of generating thermostabilized proteins makes this

strategy less appealing to membrane protein crystallographers. Typically, each residue in the protein structure is mutated to alanine, whereas natural alanine is mutated into leucine, and most stabilizing mutants are combined together to identify a particular conformation, which increases the thermostability of the target protein and favors its crystallization [121].

The crystal structures of adenosine A_{2A} receptor ($A_{2A}R$) [122], neurotensin receptor (NTSR1) [123], chemokine receptor (CCR5) [124], free fatty acid receptor (FFA1R) [125], corticotrophin release factor receptor (CRF1R) [126], and metabotropic glutamate receptor (mGlu5) [127] represent only a few examples of GPCRs, whose structures have been determined using this technique. For a complete list of thermostabilized GPCRs, please refer to [128] (or https://gpcrdb.org/construct/mutations). Although GPCRs are the main class of membrane proteins, which have been the subject of thermostabilization by mutagenesis, this technique is equally applicable to other classes of membrane proteins. This methodology has been essential for obtaining the high-resolution crystal structures of dopamine transporter [129], AMPA receptor ion channel [130], and multidrug transporter LmrP [131].

4. Assessing the homogeneity and purity of protein samples

The success of protein crystallization efforts is highly dependent on the level of protein purity and homogeneity. There are various methods to assess the quality of protein samples that are extensively used in protein production and crystallization pipelines.

4.1 UV-vis and fluorescence spectroscopy

This technique is not only used for the quantitative measurement of protein concentration but also used to detect nonprotein contaminates and protein aggregates. Amino acids such as tryptophan and tyrosine have an absorption maximum at 280 nm because of their aromatic nature, which can be exploited for measuring protein concentration using their extinction coefficients. In contrast, nucleic acids have absorption signatures at around 260 nm. A high 260/280 nm absorbance (>0.57) indicates the DNA/RNA contamination of protein samples. Large aggregates and particles in protein samples can also be detected through UV-vis spectroscopy (if their hydrodynamic radius is >200 nm). The samples without aggregates or large particles do not have any absorption beyond 320 nm, whereas the presence

of the aggregates leads to scattering of light. Besides UV spectroscopy, fluorescence spectroscopy is also used to evaluate the degree of aggregation in a protein sample. Through excitation at 280 nm, the emission signal can be monitored at 280 and 340 nm, correlated with light scattering and intrinsic protein fluorescence, respectively. The ratio of the intensities at 280 and 340 nm (I_{280}/I_{340}) corresponds to the degree of aggregation of the sample. The I_{280}/I_{340} is close to zero in the aggregation-free sample [132,133].

4.2 Size exclusion chromatography

SEC is another technique commonly used to assess the quality and homogeneity of protein samples. It is usually the last step of the protein purification process, which separates molecules according to their hydrodynamic size, often defined by their hydrodynamic radius. An SEC column is composed of a porous matrix of spherical particles (beads) that do not possess reactivity and adsorptive properties. In this technique, molecules larger than the pore size do not diffuse into the beads, so they elute early, and molecules that can penetrate the pores experience various migration times based on their size and thereby elute at different retention times. SEC is also useful for separating different oligomeric forms of a protein as well as large aggregates, which might interfere with the crystal formation. These species can be detected easily using traditional UV detectors [132]. It is crucial to remember that SEC can dilute a protein sample approximately tenfold and therefore alter the equilibration between various oligomerization states of a protein sample. In addition, although SEC possesses a porous matrix with no reactivity and absorptivity, in some cases, the protein might interact with the column matrix. Therefore, the size calculated based on running standard samples might not reflect the true size of the protein [134].

4.3 Dynamic light scattering

Dynamic light scattering (DLS) is a rapid and convenient technique to investigate the monodispersity of a protein sample and evaluate the presence of higher-order oligomers and soluble aggregates. DLS determines the size distribution of the particles, including proteins, polymers, micelles, vesicles, and so on, by measuring their Brownian motion. This technique measures the macromolecule's fluctuations in scattered light intensity as a result of diffusing particles. DLS shows the particle population at different diameters. If the system is monodispersed, only one population exists, whereas a polydispersed system would demonstrate multiple particle populations. The

advantage of DLS is that it can be performed at various temperatures and times to assess protein stability and can be performed using various buffers during the optimization steps and sample preparation. The method requires a very small amount of protein sample (0.5–2 mL, 0.3–50 mg mL^{-1}) [19]. DLS can also be coupled with SEC to understand the size distribution of protein samples [132,135,136].

4.4 Size exclusion chromatography with multiangle light scattering (SEC-MALS)

Determining the oligomeric state of proteins is essential for structural studies. In some cases, the goal is to produce the monomeric form of a protein, and in some others, the oligomeric state is desirable because certain proteins are typically active in their oligomeric forms. On the other hand, nonnative oligomers can be detrimental to structural determination by X-ray crystallography. In addition, nonnative oligomers can lead to inaccuracies in binding measurements using functional assays such as isothermal titration calorimetry (ITC) and SPR. In these cases, SEC with multiangle light scattering (SEC-MALS) can be a useful technique to determine the exact molecular mass of proteins and separate various oligomeric states. This provides a significant advantage over SEC. The size estimation by SEC can be inaccurate because the retention time in this technique mainly relies on the hydrodynamic radius of macromolecules instead of their molecular mass. Also, as mentioned earlier, proteins and other macromolecules might interact with the matrix of the SEC column, or they can adopt various conformations making the measurement of their absolute size and molar mass by running standard proteins arduous. An alternative technique is to combine SEC with MALS and differential refractive index (dRI) detectors. In SEC-MALS, the SEC column is employed only to resolve different species in solution as they enter the MALS. The dRI detector calculates the concentration using changes in the refractive index because of the analyte. At the same time, the MALS detector can measure the proportion of light scattered by an analyte at multiple angles relative to the incident laser beam. This feature enables the measurement of molecular mass independent of elution time [132,137].

5. New crystallization methods

Protein crystallization is a multiparameter process. It is divided into three steps that begin with nucleation, then the crystal growth stage, and last, cessation of growth. These steps determine the number, size, and quality of

obtained crystals. For a protein to precipitate from the solution, the system should be driven into a supersaturated state. The attainment of the supersaturation level and the rate of supersaturation can be explored on the basis of various crystallization techniques. For soluble proteins, there are four major approaches for obtaining supersaturation: vapor diffusion, batch, dialysis, and free interface diffusion (FID) [138]. In the case of membrane proteins, crystallization can be performed using LCP and bilayered bicelle crystallization methods. Each technique influences protein crystallization differently, even though the final chemical composition of the crystal system might be the same. The lack of generalized methods for high-quality crystal production is still a major bottleneck. The development of methods to control protein nucleation and crystal growth might significantly help to reduce this hurdle in the crystallization process. Now, we will discuss the most recently developed strategies to improve the crystallization process.

5.1 Automation of crystallization

Crystallization screening is the most time- and sample-consuming process in macromolecular crystallography. Because of numerous parameters to be tested, from precipitant, temperature, and pH to protein concentration, the crystallization trial is unlimited. Moreover, in some cases, crystallization is incorrectly considered an art rather than a science because of lower reproducibility and difficulty in obtaining well-diffracting crystals. Over the past decade, several automated platforms for high-throughput crystallization screening were developed to reduce manual work and increase reproducibility with a lower failure rate [139–141]. These developments include the steps from crystallization setup to drop observation. One such fully automated system is the protein crystallization and monitoring system (PXS), which has made an outstanding contribution to achieving high-throughput protein crystallization screening [139]. So far, the most commonly used crystallization method is vapor diffusion owing to its small sample volume requirement to optimize crystallization screening and easy harvesting of crystals. The drop size can vary from 50 to 1000 nL with varying parameters to set up the plates [142]. There are two types of automation robots used for setting up vapor diffusion experiments. Both robots can set up drops by mixing protein and precipitant volumes, but one can also transfer mother liquor from deep-well blocks to the plate. This avoids the extra step of setting prefilled plates by hand or another robot [143]. Similar automated systems are available for the batch crystallization process, where the protein and precipitant are dispensed simultaneously, either with or without oil [144]. Unlike

vapor diffusion, this method provides slow equilibration of the drop. However, there is no endpoint in this experiment, and the drop continues to evaporate until it dries out. This method helps to understand the phase diagram of a protein in depth. Because of their unique setup, dialysis and the interface diffusion method cannot be automated.

LCP and bicelle crystallization are preferred methods for crystallizing membrane proteins, which otherwise cannot crystallize in an aqueous phase [145]. In the standard LCP technique, membrane protein is transferred into the LCP by mixing the protein solution with lipids such as monoacylglycerols (MAGs) in an optimum ratio that might vary with the protein sample. Because of their lower chemical stability, MAGs affect crystal growth and nucleation. Recently, various research groups have been designing and synthesizing new lipids to support crystallization by forming LCP [146–149]. Because LCP is a semisolid material with high viscosity, a specialized small-diameter syringe system is used to dispense the sample in a crystallization plate [19]. Unlike soluble proteins, there are specialized automatic dispensers such as Gryphon LCP (Art Robbins), NTX (Formulatix), and Mosquito LCP (TTP LabTech) that rapidly and accurately dispense LCP to a 96-well plate. Once LCP is dispensed, the aqueous solution is added over eight wells at a time, leading to approximately 10 s exposure of these drops before being covered by the aqueous phase. To improve this, Oryx LCP (Douglas Instruments) can be used, which dispenses one LCP bolus and then the aqueous solution over it at a time within 1 s. This system can also be used for the bicelle crystallization method setup. There are a few other improvised systems, such as NT8 and ProCrys Meso Plus (Zinner Analytic), with built-in humidifiers to avoid evaporation.

With improvements in data collection and processing at beamlines, there has been a huge demand to develop a fully automated crystallization setup for the structure determination process. Recently, a new database system, PXS2, was developed to integrate the crystallization setup database with a database for the diffraction data collection on the photon factory (PF) synchrotron beamlines [150]. This system will also enable in situ data collection along with a minimized sample volume up to 0.1 mL and improved resolution of captured images. This upgraded system will significantly improve the MX efficiency in structural biology research.

5.2 On-chip crystal growth

Microfluidic devices, because of low sample consumption, finely control mass transport properties, with a large surface-area-to-volume ratio, and

have emerged as a viable technology for protein crystallization and in situ X-ray diffraction experiments [151]. Miniaturization of experiments at a small scale also facilitates good control over crystallization parameters such as temperature, concentration gradients, and convection [152,153]. These devices are also suitable for studying protein phase diagrams and understanding the crystallization process in depth by using protein samples of only a few nanoliters to microliters [153,154].

Various innovative approaches are reported that enable these devices to investigate soluble [155,156] and membrane protein crystallization [157,158]. In general, there are three types of microfluidic approaches employed to identify optimum conditions for protein crystallization: (i) valve-based systems, (ii) droplet-based systems, and (iii) well-based systems. Primarily, vapor diffusion, microbatch, and free interface methods have been used for crystallization setup on microfluidic devices. A review explained the implementation of traditional crystallization methods (microbatch, vapor diffusion, and FID) in microfluidic devices by using the three approaches mentioned earlier [159]. To perform vapor diffusion, both valve- and droplet-based approaches can be used. The first approach relies on a formulator module to create a mixture of protein and precipitant and on a two-phase injector to generate small droplets encapsulated in an immiscible carrier fluid [160]. The second droplet-based approach generates alternating protein trial droplets and salt droplets. A fluorinated carrier fluid transports and separates the droplets. Batch crystallization is performed similar to the droplet-based approach, as explained above, using a fluorinated carrier fluid. All components pass through different aqueous channels to meet at a junction and form a nanoliter volume droplet [161]. Because the carrier fluid is separated for all the aqueous solutions, no evaporation or loss of chemicals occurs, unlike the conventional crystallization method. In the case of FID, a valve-based formulator was developed to carefully manipulate the diffusion of fluids in nanoliter volumes [155]. Diffusion times between the sample and precipitant can be varied by changing the connecting channel length, which enables rational crystallization screening using on-chip FID [162].

Another crystallization method that has been explored is dialysis, which enables precise control over crystallization conditions by using a semipermeable membrane with a molecular weight cutoff (MWCO) smaller than the size of the protein of interest. There are different approaches to combining membranes and microfluidics. The most commonly used method is the direct integration of membranes into microfluidic devices by gluing or clamping. Microfluidic dialysis setups have been used for SAXS and

fluorescence recovery after photobleaching (FRAP) [163,164]. Structural changes in protein dynamics can be studied by combining microfluidic dialysis with a SAXS/UV exposure cells, and all this is possible by using a small amount of protein sample [163]. Recently, reusable microfluidic dialysis setups for in situ serial X-ray crystallography experiments have been developed. These microfluidic chips were also used for screening crystallization conditions to investigate temperature-precipitant concentration phase diagrams [165]. Such experiments open the possibilities of on-chip serial crystallography experiments under dynamically controllable sample conditions.

So far, the well-based microfluidic approach is one of the most adapted platforms for on-chip crystallization. The most recent development is the use of a triple-gradient generator device to screen the crystallization conditions for three different proteins [166]. There are other microfluidic approaches, such as a capillary-based microfluidic device that not only enables soaking of crystals at room temperature and in situ data collection but also allows stable sample shipping to synchrotrons [167]. This work paves the way for room-temperature microfluidics-based sample delivery methods to facilitate the automated workflow of high-throughput protein-crystallography-based screening of compounds for drug discovery. Various groups have attempted room-temperature serial crystallography and in situ data collection using a microfluidic device [168–172]. Lower mosaicity and good isomorphism in crystallographic data have also been observed by using microfluidic devices. Moreover, triggering events (such as light, temperature, etc.) can be easily enabled by fluidic control to investigate protein dynamics that would otherwise be inaccessible or difficult to study [170]. To mitigate radiation damage, complete crystallographic data using a microfluidic device have been collected under cryogenic temperature using lysozyme protein crystals [173], thus providing a solution for data collection of complex proteins under cryogenic conditions instead of room temperature.

For membrane protein crystallization, there are additional factors such as the presence of detergents or viscous LCP that can be challenging to form on-chip in a small volume. Because of this, the microfluidic system has been limited to detergent-based membrane protein crystallization [157,174]. A hybrid droplet-based approach that uses nanoliter plugs to minimize sample consumption has been utilized in crystallization trials of a porin from *Rhodobacter capsulatus*. In situ data collection was performed using the same approach giving high-quality crystallographic data [157]. A microfluidic device to investigate the phase behavior of sarco(endo)plasmic reticulum

Ca^{2+} adenosine triphosphatase (SERCA) has also been attempted previously, which showed the feasibility of membrane protein crystallization using microfluidic technology [174]. Droplet-based microfluidic systems have been suitable for handling viscous solutions such as LCP. This system was used to dispense nanoliter volume LCP droplets and later merged them with aqueous droplets to perform crystallization trials on bacteriorhodopsin (*Halobacterium salinarum*) [175]. They also developed a cyclodextrin-based host-guest chemistry approach in a microfluidic device. This simplified the process of protein concentration by removing free detergent micelles and thus affecting the packing of protein-detergent complexes. A time-controlled removal of loosely bound detergent molecules could also be enabled by this approach. Another microfluidic system with pneumatic valves was also used to form LCP on-chip with a droplet volume below 20 nL [176]. Implementation of current microfluidic devices is still limited to soluble proteins and should be further focused on studying membrane proteins. An improved imaging system, optimized modifications in terms of detergents, and a reliable database system can increase the number of solved membrane protein structures [159].

Microfluidic devices have emerged as a powerful tool in protein crystallization. The use of microchips has facilitated low sample and reagent consumption with a high density of experiments. This technology has revolutionized membrane protein crystallization by miniaturizing screening trials, a high operational speed, and good reproducibility. A step further was given by generating microchips with new materials such as a copolymer of cyclic olefin for in situ data collection from crystals obtained by counterdiffusion [177]. Furthermore, other advances in microfluidics are expected to mitigate radiation damage of protein crystals under the beam from a deeper understanding of the chemistry inside irradiated crystals [178].

6. New crystallization additives

Nucleation is the first step of the crystallization process that can be homogeneous or heterogeneous. A homogeneous process is a random process where multiple nuclei are formed with a simultaneous assembly of several protein molecules at a high supersaturation level. The energy barrier is low in this state, facilitating critical nuclei formation. If there is excessive supersaturation, it leads to unfavorable structural defects and excessive nucleation. To avoid this, heterogeneous nucleation is promoted to perform crystallization in a controlled manner.

The major challenge of protein crystallization is often the inability to obtain crystals. Even if crystals are obtained, other obstacles such as poor diffraction and reproducibility issues might occur. Various methods have been proposed to overcome this problem by controlling protein crystallization parameters (such as temperature, pH, concentration gradient, etc.), utilizing microgravity or electric field environments, or even developing advanced microfluidics platforms, as discussed previously [179]. Even though these methods have been an enormous success, they have some limitations. Thus, various nucleants came into existence, which induces heterogeneous nucleation and improves crystal diffraction quality in a very controlled manner [180]. Since then, there has been a massive debate on multiple substances treated as "universal" nucleants for protein nucleation. Some of these agents include minerals, microcrystals for seeding, natural nucleants (e.g., horsehair, human hair, cellulose), porous substances (e.g., silicon), and even charged surfaces (e.g., mica) [179].

6.1 Porous nucleants

Various porous nucleants have been developed, such as mesoporous bioactive gel glass, carbon-nanotube-based materials, and nanoporous gold nucleants. The most successful heterogeneous porous nucleant has been bioglass, also known as "Naomi's Nucleant" sold by Molecular Dimensions. Bioglass has a disordered pore distribution (2–10 nm) that promotes the nucleation of various difficult-to-crystallize proteins [181]. In principle, protein molecules would be trapped in pores, thereby encouraging them to form aggregates in crystalline order. Bioglass has been effective over a range of physical parameters such as different pH values, temperature, and varying isoelectric points of protein. Because of its flexibility, numerous target proteins have been crystallized, including a membrane protein [182]. Even though it is more convenient to use bioglass than silicon, its surface chemistry is not easy to control. Thus, carbon-nanotube-based nucleants with controlled pore distribution were developed [183]. Low-density or nonporous substances such as polystyrene divinylbenzene microspheres (SDB) are also effective nucleants [184]. They employ adsorption and desorption theory, where protein is first adsorbed at a high concentration and then desorbed at a low concentration. A higher-concentration region is favorable to nucleation, and a lower-concentration region allows crystal nuclei stability leading to the growth of high-quality protein crystals. The discovery of such effective porous materials has led to structural studies of various proteins by inducing nucleation. This has also set a trend for developing new nucleants for protein crystallization.

6.2 Molecularly imprinted polymers (MIPs)

Molecularly imprinted polymers (MIPs) are another such nucleants that produce molecularly selective sites via the polymerization of a functional monomer and a template biomolecule. There is an interaction between the functional monomer and template molecule via hydrogen bonding and weak Van der Waals forces. Once polymerized, the template molecule is trapped inside the polymer. The highly selective cavities remain after the removal of the template molecule. These cavities can remember the cognate template molecule and rebind to a noncognate molecule of a similar shape and size [185,186]. MIPs have been successfully used as a nonprotein nucleant in protein crystallization. They are very effective in increasing crystal hits and improving crystal quality. The first water-based MIP (HydroMIP), also known as 'smart material', was developed by Naomi Chayen in 2011 [187]. The most commonly used MIPs are acrylamide (AA), *N*-hydroxymethyl acrylamide (NHMA), and N-isopropyl acrylamide (NiPAm). To prepare MIPs, a functional monomer (i.e., AA) and a crosslinker (i.e., N,N0-methylenebisacrylamide) are dissolved in deionized water to form a pre-MIP solution. The solution is then polymerized by adding ammonium persulphate (APS) and *N,N,N, N*-tetramethylethyldiamine (TEMED) at room temperature. Last, formed gels are crushed, and the template protein molecule is removed, forming cavities. These cavities form a protein-rich phase when protein molecules migrate toward their surface. This overcomes the energy barrier for the first crystal nuclei formation step. The cavity surface is used as a support for protein crystal growth.

Various proteins such as lysozyme, catalase, hemoglobin, trypsin, alpha crustacyanin, and human macrophage migration inhibitory factor (MIF) have been tested for nucleation using MIPs [187,188]. Nucleation is induced by cognate MIP and also via other similar noncognate MIPs under metastable conditions. By using MIPs, the diffraction quality of the crystals can be improved with low protein consumption. MIPs can also be used in high-throughput automated crystallization trials and give high reproducibility [189]. To further improve the crystal quality, zwitterionic additives have been immobilized in MIPs that gave higher hits and well-diffracting single crystals of concanavalin A protein in a short time [190].

6.3 Crystallophore (Tb-Xo4)

Apart from getting high-quality protein crystals, solving the phase problem is another major issue in crystallography. For more than a decade, lanthanide

complexes have been widely used to resolve the phase problem because of their large anomalous contribution of lanthanide ions [191]. These complexes can be inserted into protein crystals by (i) substituting Ca^{2+} in calcium-binding proteins [192], (ii) by covalent grafting of a lanthanide binding tag [193], and (iii) cocrystallization of lanthanide complexes with the protein [194]. Previously, several such complexes such as macrocyclic (DOTA, DO3A, and HPDO3A), polydentate (DTPA-BMA), or tris-dipicolinate lanthanide complexes have been used for the structural determination of new proteins [195,196].

Recently, a new terbium (III) complex (cationic) has been developed that has all the properties such as nucleating, phasing, and luminescence to overcome major issues of macromolecular crystallography. Engilberge et al. named this type of complex as crystallophore (Xo4), which has been used for the structural determination of various proteins with known and unknown structures (such as lysozyme, thaumatin, malate dehydrogenase, and pb9 from the T5 phage tail) [197]. It has been proposed that nucleating properties of Tb-Xo4 could be because of SER or by a slight modification of the surface topology favoring a contact between protein molecules. This complex is highly stable under crystallization conditions and acts as a good phasing agent enabling the protein structure determination using single-wavelength anomalous diffraction (SAD) or multiwavelength anomalous diffraction (MAD) methods. The addition of this crystallophore also improved the diffraction quality and gave greater data completeness, as observed previously for an adhesion protein PitA [198]. The use of heavy atoms to solve phasing problems has recently become popular, and a new Gd(III) clathrochelate, a metal cage complex, has been designed by Castañeda et al. [199]. Tb-Xo4 has huge potential in facilitating the structural elucidation of new proteins with its capabilities to overcome issues such as phasing and crystal nucleation. In the future, it will be interesting to see this crystallophore's compatibility in phasing tools with serial crystallography.

6.4 Other nucleants

Natural nucleants such as hair are preferred because of their biocompatibility and easy availability. Mineral substances have also shown superior results. Previously, nucleation of four different proteins and crystal growth were observed using different mineral samples as nucleants [200]. However, they altered the crystal morphology and unit cell symmetry [201]. Porous substances such as silicon have also demonstrated crystal formation in the

metastable zone for various proteins. The silicon pore size is similar to protein's molecular size in the crystalline form. Thus, these pores might trap protein molecules to induce crystal nucleation [202].

7. Advances in instrument and data-processing software

7.1 Automations in screening crystallization conditions

Following advances in X-ray radiation sources, technologies related to mounting and storing crystals, postdiffraction data processing programs, and obtaining phases are booming. One of these advances is automating the crystallization process from preparing conditions to sample dispensing. The focus of automation technologies for protein crystallization majored in two independent approaches: the robotic systems equipped with microdispensing heads and microfluidic chips with parallel valves [203]. Phoenix (Art Robbins Instruments, Inc.), Mosquito (TTP Labtech, Ltd.), Oryx Nano (Douglas Instruments, Ltd.), and NT8 (Formulatrix, Inc.) are some examples of the automated robots that can dispense and mix protein and crystallization solutions to the smallest volumes (nanoliter scales). High reliability, high throughput, low sample usage, and complete automation are prominent advantages of using these robots [204]. Microfluidic devices have also been developed in various designs to handle a small amount of liquids for different crystallization setups. In one of the designs, groups of microvalves were incorporated on a chip to combine the mixtures of proteins and crystallization solutions rapidly in a formulation chip or generate volume-defined microchambers for mixing nanoliter scales of proteins through an array of pneumatic valves [205].

7.2 Detecting protein crystals using an automated plate imager

The new instrumental advancement allows crystallization plates to be stored in a RockImager (Formulatrix, Bedford, MA, USA) for automated storage and imaging. In this approach, one can monitor the crystal growth while maintaining the plates at a constant temperature according to a schedule determined by the user. Periodic imaging of individual drops on each plate is performed to monitor the crystallization process. The RockImager system can store 1000 plates at once and image them according to the schedule. The images of drops, conditions for each drop, and the user experimental notes are all available on a server database pertinent to the imaging system. Using the RockMaker software, the users can monitor and score the drops from 0

to 9, starting from the clear drop and dust to crystals and marking the ones containing crystals as interesting drops. RockImager is also capable of distinguishing between protein and salt crystals. Tryptophan shows a high quantum yield when it gets excited at around 290 nm, which makes it useful as a fluorescent probe. On average, 1.09% of the residues in proteins constitute tryptophan, which provides a sufficient fluorescence signal for UV imaging. A protein crystal can be easily distinguished in UV images even when the crystals are buried under heavy precipitation. It must be noted that this technique has several limitations that have been reviewed thoroughly elsewhere [206,207].

7.3 Advances in synchrotron radiation instrumentation

Most X-ray crystal structures deposited in the PDB have been collected using synchrotrons because of the transition to high-brightness, third-generation synchrotron radiation sources. The European Synchrotron Radiation Facility (ESRF) was one of the earliest generations of these synchrotrons. Shortly afterward, Advanced Photon Source (APS) in USA and Spring 8 in Japan (Super Photon Ring 8GeV) launched their activities. The highly intense X-ray beams in ESRF, APS, and Spring 8 are achieved using X-ray undulators. Another essential feature of these undulators is a tunable X-ray wavelength that alters the magnet gap. New generations of synchrotrons offer much smaller, focused beams that allow the measurement of X-ray diffraction data for microcrystal samples [208]. Additionally, other experiments, such as optimized anomalous dispersion measurement or phasing, data collection for large unit cells, and high-resolution measurements, are now amenable through a much smaller number of crystals and much shorter recording times. Furthermore, robotics has become quite a standard method for handling samples, and in most synchrotron locations, one only needs to ship the crystals using a dry-shipper to the site, and all the handling can be performed remotely.

The detectors for synchrotron X-ray diffraction have also been advanced from photographic film to TV systems, imaging plates, charge-coupled devices (CCDs), and pixel detectors. These advancements have led to faster data collection at synchrotrons than home source X-ray generators [209–211].

7.4 In situ X-ray screening and data collection

As mentioned earlier, one of the methods to distinguish protein versus salt crystals is to use UV fluorescence and second-order harmonic generation

techniques [206]. However, X-ray screening not only identifies protein versus salt crystals but also provides data collection-related information, including space group, unit cell, and diffraction quality. Therefore, in situ screening speeds up the crystallization screening pipeline to determine the diffraction-based optimal conditions and ligand binding state. This can be highly beneficial for drug discovery applications [212,213]. Also, in experiments such as serial crystallography, where many crystals are required, harvesting that many crystals become almost impossible, and an in situ experiment is a major tool [214]. In situ data collection is executed mostly at room temperature. The room-temperature data collection allows time-resolved experiments for probing chemical reactions in the crystals. The disadvantage of this method is that the data collection at room temperature increases the mosaicity of crystals during the data collection. New advances in in situ sample preparation, such as utilizing thin-film samples, enable the flash-cooling of in situ samples and data collection under cryogenic conditions [215].

7.5 In situ data collection using X-ray free-electron laser (XFEL)

The cryocooling of samples decreases the rate of secondary damage stemming from the ionizing radiation. However, it has been shown that X-ray damage can also be omitted by employing very short X-ray pulses comprising fewer than 100-fs intervals. The "diffraction-before-destruction" principle enables the collection of diffraction data from very small protein crystals before they deteriorate through extremely bright and short X-ray pulses [216]. Several X-ray free-electron laser (XFEL) sources have been established around the world, such as the linac coherent light source (LCLS) in Menlo Park, USA, Spring-8 Angstrom Coherent Laser (SACLA) in Harima, Japan, PAL-XFEL in Pohang, South Korea, the European XFEL in Hamburg, Germany, and SwissFEL in Villigen, Switzerland. These sources can generate coherent X-rays with energies up to ~13 keV (25 keV for some sources) and a peak brilliance of about 9–10 orders of magnitude stronger than a third-generation synchrotron [217].

XFEL provides an excellent platform for time-resolved experiments [218] to elucidate the mechanism of proteins and enzymes in subpicosecond time scales. Recently, Nogly et al. visualized the early step of photoisomerization of retinal in bacteriorhodopsin using a pump-probe technique. Their study initiated the excitation of BR microcrystals through optical laser

pulses (pump), and the microcrystals were injected across the femtosecond X-ray pulses (probe). They elucidated the microenvironment of proteins that drives the photoisomerization of retinal during and after the excitation of the chromophore [219].

7.6 The computational tools available in protein crystallography

Since the early days of protein crystallography, the instruments for X-ray data collection and the software employed in data processing have undergone tremendous improvements. The data collection process has been programmed into an automatic process, whereas the accuracy of these processes depends upon the quality of the integration and scaling software. Three software packages are mainly employed for processing the diffraction data: iMosflm (part of the CCP4 suite), HKL2000, and HKL3000 (comprising the integration program Denzo as well as merging and scaling the program Scalepack) and the XDS suite (containing programs for both scaling and integration) [220].

DIALS is another software for data processing for synchrotrons and XFELs; however, it does not perform scaling or merging tasks. The software's automated data collection pipelines enable the user to acquire an optimal data collection strategy, collect high-quality data, and complete the dataset for each crystal. To process the more complex datasets, graphical user interfaces (GUIs) allow manual processing. All recent interfaces provide a general workflow of reading diffraction images, finding spots for indexing, indexing the spots, refining the crystal and detector parameters, integrating the diffraction maxima, and scaling, merging, or exporting the reflection files [221]. Two major protein crystallography software for data quality assessment, model and ligand building, phasing, refinements, and so on are Collaborative Computational Project Number 4 (CCP4) and Python-based Hierarchical Environment for Integrated Crystallography (Phenix) [222], which are extensively used in solving X-ray and cryo-EM protein structures. In addition, various model viewers such as Coot [219], PyMol, and UCSF Chimera [223] have been developed for visualizing protein structures and generating high-quality graphics.

8. Conclusions and future perspectives

The emergence of new technologies such as XFEL, neutron diffraction, and Micro-ED is expanding the toolkit necessary for obtaining the

high-resolution structure of target proteins. Although XFEL requires nano-size protein crystals to be continuously delivered at room temperature, neutron diffraction uses perdeuterated millimeter-sized crystals, and Micro-ED requires micrometer-sized crystals under cryogenic conditions. This diversity in techniques encourages the demand for a better understanding and reproducibility of the biomolecular crystallization process. Meanwhile, new technological advances are introduced to meet the requirement of this diversity of crystal sizes for various diffraction techniques. However, with the advent of pulsed neutron sources such as ESS, the need for large crystals might reduce as the labeling methods for sample preparation are improving [224]. Devices capable of producing short pulses of X-rays are developed, which are far brighter than the radiation pulses generated by current synchrotrons. This will further revolutionize the field of structural biology, where one could get away with very small-size crystals. Other technological advances include cryo-electron tomography (cryo-ET), which enables the investigation of the molecular architecture of protein complexes within the native cell. These assist scientists in understanding fundamental key cell processes and building the image of inner cell structures. During the past decade, microfluidic devices (microchips) have also emerged as a powerful tool in protein crystallization. They enable the miniaturization of crystallization experiments using sample volumes much smaller than the sample volume necessary for current robotic systems. It is anticipated that microfluidic devices will play a central role in protein crystallization studies ranging from screening and crystal improvement to in situ data collection in the near future.

References

[1] Kendrew JC, Bodo G, Dintzis HM, Parrish RG, Wyckoff H, Phillips DC. A three-dimensional model of the myoglobin molecule obtained by X-ray analysis. Nature 1958;181:662–6. https://doi.org/10.1038/181662a0.

[2] Perutz MF, Rossmann MG, Cullis AF, Muirhead H, Will G, North AC. Structure of haemoglobin: a three-dimensional Fourier synthesis at 5.5-A resolution, obtained by X-ray analysis. Nature 1960;185:416–22. https://doi.org/10.1038/185416a0.

[3] Crowther RA, Klug A. Structural analysis of macromolecular assemblies by image reconstruction from electron micrographs. Annu Rev Biochem 1975;44:161–82. https://doi.org/10.1146/annurev.bi.44.070175.001113.

[4] Deisenhofer J, Epp O, Miki K, Huber R, Michel H. X-ray structure analysis of a membrane protein complex. Electron density map at 3 A resolution and a model of the chromophores of the photosynthetic reaction center from *Rhodopseudomonas viridis*. J Mol Biol 1984;180:385–98. https://doi.org/10.1016/s0022-2836(84)80011-x.

[5] Abrahams JP, Leslie AG, Lutter R, Walker JE. Structure at 2.8 A resolution of F1-ATPase from bovine heart mitochondria. Nature 1994;370:621–8. https://doi.org/10.1038/370621a0.

[6] Doyle DA, Morais Cabral J, Pfuetzner RA, Kuo A, Gulbis JM, Cohen SL, Chait BT, MacKinnon R. The structure of the potassium channel: molecular basis of K+ conduction and selectivity. Science 1998;280:69–77. https://doi.org/10.1126/science.280.5360.69.
[7] Cramer P, Bushnell DA, Kornberg RD. Structural basis of transcription: RNA polymerase II at 2.8 angstrom resolution. Science 2001;292:1863–76. https://doi.org/10.1126/science.1059493.
[8] Rasmussen SG, Choi HJ, Rosenbaum DM, Kobilka TS, Thian FS, Edwards PC, Burghammer M, Ratnala VR, Sanishvili R, Fischetti RF, Schertler GF, Weis WI, Kobilka BK. Crystal structure of the human beta2 adrenergic G-protein-coupled receptor. Nature 2007;450:383–7. https://doi.org/10.1038/nature06325.
[9] Krogh A, Larsson B, von Heijne G, Sonnhammer ELL. Predicting transmembrane protein topology with a hidden markov model: application to complete genomes 11 edited by F. Cohen. J Mol Biol 2001;305:567–80. https://doi.org/10.1006/jmbi.2000.4315.
[10] Rask-Andersen M, Almen MS, Schioth HB. Trends in the exploitation of novel drug targets. Nat Rev Drug Discov 2011;10:579–90. https://doi.org/10.1038/nrd3478.
[11] Santos R, Ursu O, Gaulton A, Bento AP, Donadi RS, Bologa CG, Karlsson A, Al-Lazikani B, Hersey A, Oprea TI, Overington JP. A comprehensive map of molecular drug targets. Nat Rev Drug Discov 2017;16:19–34. https://doi.org/10.1038/nrd.2016.230.
[12] Palczewski K, Kumasaka T, Hori T, Behnke CA, Motoshima H, Fox BA, Trong IL, Teller DC, Okada T, Stenkamp RE, Yamamoto M, Miyano M. Crystal structure of rhodopsin: a G protein-coupled receptor. Science 2000;289:739. https://doi.org/10.1126/science.289.5480.739.
[13] Cherezov V, Rosenbaum DM, Hanson MA, Rasmussen SGF, Thian FS, Kobilka TS, Choi H-J, Kuhn P, Weis WI, Kobilka BK, Stevens RC. High-resolution crystal structure of an engineered human beta2-adrenergic G protein-coupled receptor. Science (New York, NY) 2007;318:1258–65. https://doi.org/10.1126/science.1150577.
[14] Rasmussen SGF, Choi H-J, Rosenbaum DM, Kobilka TS, Thian FS, Edwards PC, Burghammer M, Ratnala VRP, Sanishvili R, Fischetti RF, Schertler GFX, Weis WI, Kobilka BK. Crystal structure of the human β2 adrenergic G-protein-coupled receptor. Nature 2007;450:383–7. https://doi.org/10.1038/nature06325.
[15] Rasmussen SG, DeVree BT, Zou Y, Kruse AC, Chung KY, Kobilka TS, Thian FS, Chae PS, Pardon E, Calinski D, Mathiesen JM, Shah ST, Lyons JA, Caffrey M, Gellman SH, Steyaert J, Skiniotis G, Weis WI, Sunahara RK, Kobilka BK. Crystal structure of the beta2 adrenergic receptor-Gs protein complex. Nature 2011;477:549–55. https://doi.org/10.1038/nature10361.
[16] Doyle DA, Cabral JM, Pfuetzner RA, Kuo A, Gulbis JM, Cohen SL, Chait BT, MacKinnon R. The structure of the potassium channel: molecular basis of K+ conduction and selectivity. Science 1998;280:69. https://doi.org/10.1126/science.280.5360.69.
[17] Jiang Y, Lee A, Chen J, Cadene M, Chait BT, MacKinnon R. Crystal structure and mechanism of a calcium-gated potassium channel. Nature 2002;417:515–22. https://doi.org/10.1038/417515a.
[18] Congreve M, Dias JM, Marshall FH. Structure-based drug design for G protein-coupled receptors. In: Lawton G, Witty DR, editors. Progress in medicinal chemistry. Elsevier; 2014. p. 1–63 [Chapter 1].
[19] Kermani AA. A guide to membrane protein X-ray crystallography. FEBS J 2021;288:5788–804. https://doi.org/10.1111/febs.15676.
[20] Singh DB, Tripathi T. Frontiers in protein structure, function, and dynamics. 1st. Singapore: Springer Nature; 2020. p. 1–458.
[21] Tripathi T, Dubey VK. Advances in protein molecular and structural biology methods. 1st. Cambridge, MA, USA: Academic Press; 2022. p. 1–714.

[22] Katrusiak A. High-pressure crystallography. Acta Crystallogr Sect A: Found Crystallogr 2008;64:135–48. https://doi.org/10.1107/S0108767307061181.
[23] McIlwain BC, Kermani AA. Membrane protein production in *Escherichia coli*. In: Perez C, Maier T, editors. Expression, purification, and structural biology of membrane proteins. New York, NY: Springer US; 2020. p. 13–27.
[24] Chae PS, Rasmussen SGF, Rana RR, Gotfryd K, Chandra R, Goren MA, Kruse AC, Nurva S, Loland CJ, Pierre Y, Drew D, Popot J-L, Picot D, Fox BG, Guan L, Gether U, Byrne B, Kobilka B, Gellman SH. Maltose-neopentyl glycol (MNG) amphiphiles for solubilization, stabilization and crystallization of membrane proteins. Nat Methods 2010;7:1003–8. https://doi.org/10.1038/nmeth.1526.
[25] Chung KY, Kim TH, Manglik A, Alvares R, Kobilka BK, Prosser RS. Role of detergents in conformational exchange of a G protein-coupled receptor. J Biol Chem 2012;287:36305–11. https://doi.org/10.1074/jbc.M112.406371.
[26] Chae PS, Rana RR, Gotfryd K, Rasmussen SGF, Kruse AC, Cho KH, Capaldi S, Carlsson E, Kobilka B, Loland CJ, Gether U, Banerjee S, Byrne B, Lee JK, Gellman SH. Glucose-neopentyl glycol (GNG) amphiphiles for membrane protein study. Chem Commun (Camb) 2013;49:2287–9. https://doi.org/10.1039/c2cc36844g.
[27] Sharma KS, Durand G, Gabel F, Bazzacco P, Le Bon C, Billon-Denis E, Catoire LJ, Popot J-L, Ebel C, Pucci B. Non-ionic amphiphilic homopolymers: synthesis, solution properties, and biochemical validation. Langmuir 2012;28:4625–39. https://doi.org/10.1021/la205026r.
[28] Matar-Merheb R, Rhimi M, Leydier A, Huché F, Galián C, Desuzinges-Mandon E, Ficheux D, Flot D, Aghajari N, Kahn R, Di Pietro A, Jault J-M, Coleman AW, Falson P. Structuring detergents for extracting and stabilizing functional membrane proteins. PLoS One 2011;6, e18036. https://doi.org/10.1371/journal.pone.0018036.
[29] Frotscher E, Danielczak B, Vargas C, Meister A, Durand G, Keller S. A fluorinated detergent for membrane-protein applications. Angew Chem Int Ed Eng 2015;54:5069–73. https://doi.org/10.1002/anie.201412359.
[30] Rosenbaum DM, Zhang C, Lyons JA, Holl R, Aragao D, Arlow DH, Rasmussen SGF, Choi H-J, DeVree BT, Sunahara RK, Chae PS, Gellman SH, Dror RO, Shaw DE, Weis WI, Caffrey M, Gmeiner P, Kobilka BK. Structure and function of an irreversible agonist-β2 adrenoceptor complex. Nature 2011;469:236–40. https://doi.org/10.1038/nature09665.
[31] Kruse AC, Hu J, Pan AC, Arlow DH, Rosenbaum DM, Rosemond E, Green HF, Liu T, Chae PS, Dror RO, Shaw DE, Weis WI, Wess J, Kobilka BK. Structure and dynamics of the M3 muscarinic acetylcholine receptor. Nature 2012;482:552–6. https://doi.org/10.1038/nature10867.
[32] White JF, Noinaj N, Shibata Y, Love J, Kloss B, Xu F, Gvozdenovic-Jeremic J, Shah P, Shiloach J, Tate CG, Grisshammer R. Structure of the agonist-bound neurotensin receptor. Nature 2012;490:508–13. https://doi.org/10.1038/nature11558.
[33] Rollauer SE, Tarry MJ, Graham JE, Jääskeläinen M, Jäger F, Johnson S, Krehenbrink M, Liu S-M, Lukey MJ, Marcoux J, McDowell MA, Rodriguez F, Roversi P, Stansfeld PJ, Robinson CV, Sansom MSP, Palmer T, Högbom M, Berks BC, Lea SM. Structure of the TatC core of the twin-arginine protein transport system. Nature 2012;492:210–4. https://doi.org/10.1038/nature11683.
[34] Paulsen CE, Armache J-P, Gao Y, Cheng Y, Julius D. Structure of the TRPA1 ion channel suggests regulatory mechanisms. Nature 2015;520:511–7. https://doi.org/10.1038/nature14367.
[35] Yin J, Mobarec JC, Kolb P, Rosenbaum DM. Crystal structure of the human OX2 orexin receptor bound to the insomnia drug suvorexant. Nature 2015;519:247–50. https://doi.org/10.1038/nature14035.
[36] Kang Y, Zhou XE, Gao X, He Y, Liu W, Ishchenko A, Barty A, White TA, Yefanov O, Han GW, Xu Q, de Waal PW, Ke J, Tan MHE, Zhang C, Moeller A, West GM,

Pascal BD, Van Eps N, Caro LN, Vishnivetskiy SA, Lee RJ, Suino-Powell KM, Gu X, Pal K, Ma J, Zhi X, Boutet S, Williams GJ, Messerschmidt M, Gati C, Zatsepin NA, Wang D, James D, Basu S, Roy-Chowdhury S, Conrad CE, Coe J, Liu H, Lisova S, Kupitz C, Grotjohann I, Fromme R, Jiang Y, Tan M, Yang H, Li J, Wang M, Zheng Z, Li D, Howe N, Zhao Y, Standfuss J, Diederichs K, Dong Y, Potter CS, Carragher B, Caffrey M, Jiang H, Chapman HN, Spence JCH, Fromme P, Weierstall U, Ernst OP, Katritch V, Gurevich VV, Griffin PR, Hubbell WL, Stevens RC, Cherezov V, Melcher K, Xu HE. Crystal structure of rhodopsin bound to arrestin by femtosecond X-ray laser. Nature 2015;523:561–7. https://doi.org/10.1038/nature14656.

[37] Perez C, Gerber S, Boilevin J, Bucher M, Darbre T, Aebi M, Reymond J-L, Locher KP. Structure and mechanism of an active lipid-linked oligosaccharide flippase. Nature 2015;524:433–8. https://doi.org/10.1038/nature14953.

[38] Taniguchi R, Kato HE, Font J, Deshpande CN, Wada M, Ito K, Ishitani R, Jormakka M, Nureki O. Outward- and inward-facing structures of a putative bacterial transition-metal transporter with homology to ferroportin. Nat Commun 2015;6:8545. https://doi.org/10.1038/ncomms9545.

[39] Benton DJ, Nans A, Calder LJ, Turner J, Neu U, Lin YP, Ketelaars E, Kallewaard NL, Corti D, Lanzavecchia A, Gamblin SJ, Rosenthal PB, Skehel JJ. Influenza hemagglutinin membrane anchor. Proc Natl Acad Sci 2018;115:10112. https://doi.org/10.1073/pnas.1810927115.

[40] Gao Y, Hu H, Ramachandran S, Erickson JW, Cerione RA, Skiniotis G. Structures of the rhodopsin-transducin complex: insights into G-protein activation. Mol Cell 2019;75, 781-790.e783. https://doi.org/10.1016/j.molcel.2019.06.007.

[41] Sun J. Structures of mouse DUOX1-DUOXA1 provide mechanistic insights into enzyme activation and regulation. Nat Struct Mol Biol 2020;27:1086–93. https://doi.org/10.1038/s41594-020-0501-x.

[42] Sun J, MacKinnon R. Structural basis of human KCNQ1 modulation and gating. Cell 2020;180, 340-347.e349. https://doi.org/10.1016/j.cell.2019.12.003.

[43] Huynh KW, Cohen MR, Jiang J, Samanta A, Lodowski DT, Zhou ZH, Moiseenkova-Bell VY. Structure of the full-length TRPV2 channel by cryo-EM. Nat Commun 2016;7:11130. https://doi.org/10.1038/ncomms11130.

[44] Nishizawa T, Kita S, Maturana AD, Furuya N, Hirata K, Kasuya G, Ogasawara S, Dohmae N, Iwamoto T, Ishitani R, Nureki O. Structural basis for the counter-transport mechanism of a H^+/Ca^{2+} exchanger. Science 2013;341:168–72. https://doi.org/10.1126/science.1239002.

[45] Dong YY, Pike AC, Mackenzie A, McClenaghan C, Aryal P, Dong L, Quigley A, Grieben M, Goubin S, Mukhopadhyay S, Ruda GF, Clausen MV, Cao L, Brennan PE, Burgess-Brown NA, Sansom MS, Tucker SJ, Carpenter EP. K2P channel gating mechanisms revealed by structures of TREK-2 and a complex with Prozac. Science 2015;347:1256–9. https://doi.org/10.1126/science.1261512.

[46] Bausewein T, Mills DJ, Langer JD, Nitschke B, Nussberger S, Kühlbrandt W. Cryo-EM structure of the TOM core complex from Neurospora crassa. Cell 2017;170. https://doi.org/10.1016/j.cell.2017.07.012. 693–700.e697.

[47] Kubota-Kawai H, Burton-Smith RN, Tokutsu R, Song C, Akimoto S, Yokono M, Ueno Y, Kim E, Watanabe A, Murata K, Minagawa J. Ten antenna proteins are associated with the core in the supramolecular organization of the photosystem I supercomplex in *Chlamydomonas reinhardtii*. J Biol Chem 2019;294:4304–14. https://doi.org/10.1074/jbc.RA118.006536.

[48] Burton-Smith RN, Watanabe A, Tokutsu R, Song C, Murata K, Minagawa J. Structural determination of the large photosystem II–light-harvesting complex II supercomplex of *Chlamydomonas reinhardtii* using nonionic amphipol. J Biol Chem 2019;294:15003–13. https://doi.org/10.1074/jbc.RA119.009341.

[49] Agez M, Schultz P, Medina I, Baker DJ, Burnham MP, Cardarelli RA, Conway LC, Garnier K, Geschwindner S, Gunnarsson A, McCall EJ, Frechard A, Audebert S, Deeb TZ, Moss SJ, Brandon NJ, Wang Q, Dekker N, Jawhari A. Molecular architecture of potassium chloride co-transporter KCC2. Sci Rep 2017;7:16452. https://doi.org/10.1038/s41598-017-15739-1.

[50] Tribet C, Audebert R, Popot JL. Amphipols: polymers that keep membrane proteins soluble in aqueous solutions. Proc Natl Acad Sci U S A 1996;93:15047–50. https://doi.org/10.1073/pnas.93.26.15047.

[51] Rahmeh R, Damian M, Cottet M, Orcel H, Mendre C, Durroux T, Sharma KS, Durand G, Pucci B, Trinquet E, Zwier JM, Deupi X, Bron P, Banères J-L, Mouillac B, Granier S. Structural insights into biased G protein-coupled receptor signaling revealed by fluorescence spectroscopy. Proc Natl Acad Sci 2012;109:6733–8. https://doi.org/10.1073/pnas.1201093109.

[52] Desuzinges Mandon E, Traversier A, Champagne A, Benier L, Audebert S, Balme S, Dejean E, Rosa Calatrava M, Jawhari A. Expression and purification of native and functional influenza A virus matrix 2 proton selective ion channel. Protein Expr Purif 2017;131:42–50. https://doi.org/10.1016/j.pep.2016.11.001.

[53] Park KH, Berrier C, Lebaupain F, Pucci B, Popot JL, Ghazi A, Zito F. Fluorinated and hemifluorinated surfactants as alternatives to detergents for membrane protein cell-free synthesis. Biochem J 2007;403:183–7. https://doi.org/10.1042/bj20061473.

[54] Breyton C, Chabaud E, Chaudier Y, Pucci B, Popot JL. Hemifluorinated surfactants: a non-dissociating environment for handling membrane proteins in aqueous solutions? FEBS Lett 2004;564:312–8. https://doi.org/10.1016/s0014-5793(04)00227-3.

[55] Willegems K, Efremov RG. Influence of lipid mimetics on gating of ryanodine receptor. Structure 2018;26:1303–1313.e1304. https://doi.org/10.1016/j.str.2018.06.010.

[56] Kermani AA, Macdonald CB, Burata OE, Ben Koff B, Koide A, Denbaum E, Koide S, Stockbridge RB. The structural basis of promiscuity in small multidrug resistance transporters. Nat Commun 2020;11:6064. https://doi.org/10.1038/s41467-020-19820-8.

[57] Kermani AA, Macdonald CB, Gundepudi R, Stockbridge RB. Guanidinium export is the primal function of SMR family transporters. Proc Natl Acad Sci U S A 2018;115:3060–5. https://doi.org/10.1073/pnas.1719187115.

[58] Nikolaev M, Round E, Gushchin I, Polovinkin V, Balandin T, Kuzmichev P, Shevchenko V, Borshchevskiy V, Kuklin A, Round A, Bernhard F, Willbold D, Büldt G, Gordeliy V. Integral membrane proteins can be crystallized directly from nanodiscs. Cryst Growth Des 2017;17:945–8. https://doi.org/10.1021/acs.cgd.6b01631.

[59] Broecker J, Eger BT, Ernst OP. Crystallogenesis of membrane proteins mediated by polymer-bounded lipid nanodiscs. Structure 2017;25:384–92. https://doi.org/10.1016/j.str.2016.12.004.

[60] Denisov IG, Grinkova YV, Lazarides AA, Sligar SG. Directed self-assembly of monodisperse phospholipid bilayer nanodiscs with controlled size. J Am Chem Soc 2004;126:3477–87. https://doi.org/10.1021/ja0393574.

[61] Denisov IG, Sligar SG. Nanodiscs for structural and functional studies of membrane proteins. Nat Struct Mol Biol 2016;23:481–6. https://doi.org/10.1038/nsmb.3195.

[62] Bayburt TH, Sligar SG. Membrane protein assembly into nanodiscs. FEBS Lett 2010;584:1721–7. https://doi.org/10.1016/j.febslet.2009.10.024.

[63] Goddard AD, Dijkman PM, Adamson RJ, dos Reis RI, Watts A. Reconstitution of membrane proteins: a GPCR as an example. Methods Enzymol 2015;556:405–24. https://doi.org/10.1016/bs.mie.2015.01.004.

[64] Su C-C, Morgan CE, Kambakam S, Rajavel M, Scott H, Huang W, Emerson CC, Taylor DJ, Stewart PL, Bonomo RA, Yu EW. Cryo-electron microscopy structure of an *Acinetobacter baumannii* multidrug efflux pump. mBio 2019;10, e01295-01219.- https://doi.org/10.1128/mBio.01295-19.

[65] Postis V, Rawson S, Mitchell JK, Lee SC, Parslow RA, Dafforn TR, Baldwin SA, Muench SP. The use of SMALPs as a novel membrane protein scaffold for structure study by negative stain electron microscopy. Biochim Biophys Acta Biomembr 2015;1848:496–501. https://doi.org/10.1016/j.bbamem.2014.10.018.
[66] Phillips R, Ursell T, Wiggins P, Sens P. Emerging roles for lipids in shaping membrane-protein function. Nature 2009;459:379–85. https://doi.org/10.1038/nature08147.
[67] Guo Y. Be cautious with crystal structures of membrane proteins or complexes prepared in detergents. Crystals 2020;10. https://doi.org/10.3390/cryst10020086.
[68] Qiu W, Fu Z, Xu GG, Grassucci RA, Zhang Y, Frank J, Hendrickson WA, Guo Y. Structure and activity of lipid bilayer within a membrane-protein transporter. Proc Natl Acad Sci 2018;115:12985. https://doi.org/10.1073/pnas.1812526115.
[69] Frauenfeld J, Löving R, Armache J-P, Sonnen AFP, Guettou F, Moberg P, Zhu L, Jegerschöld C, Flayhan A, Briggs JAG, Garoff H, Löw C, Cheng Y, Nordlund P. A saposin-lipoprotein nanoparticle system for membrane proteins. Nat Methods 2016;13:345–51. https://doi.org/10.1038/nmeth.3801.
[70] Bruhn H. A short guided tour through functional and structural features of saposin-like proteins. Biochem J 2005;389:249–57. https://doi.org/10.1042/BJ20050051.
[71] Kapust RB, Waugh DS. *Escherichia coli* maltose-binding protein is uncommonly effective at promoting the solubility of polypeptides to which it is fused. Protein Sci 1999;8:1668–74. https://doi.org/10.1110/ps.8.8.1668.
[72] Smyth DR, Mrozkiewicz MK, McGrath WJ, Listwan P, Kobe B. Crystal structures of fusion proteins with large-affinity tags. Protein Sci 2003;12:1313–22. https://doi.org/10.1110/ps.0243403.
[73] Jin T, Chuenchor W, Jiang J, Cheng J, Li Y, Fang K, Huang M, Smith P, Xiao TS. Design of an expression system to enhance MBP-mediated crystallization. Sci Rep 2017;7:40991. https://doi.org/10.1038/srep40991.
[74] Bokhove M, Al Hosseini HS, Saito T, Dioguardi E, Gegenschatz-Schmid K, Nishimura K, Raj I, de Sanctis D, Han L, Jovine L. Easy mammalian expression and crystallography of maltose-binding protein-fused human proteins. J Struct Biol 2016;194:1–7. https://doi.org/10.1016/j.jsb.2016.01.016.
[75] Lieberman RL, Culver JA, Entzminger KC, Pai JC, Maynard JA. Crystallization chaperone strategies for membrane proteins. Methods 2011;55:293–302. https://doi.org/10.1016/j.ymeth.2011.08.004.
[76] Koide S. Engineering of recombinant crystallization chaperones. Curr Opin Struct Biol 2009;19:449–57. https://doi.org/10.1016/j.sbi.2009.04.008.
[77] Zhou M, Robinson CV. Flexible membrane proteins: functional dynamics captured by mass spectrometry. Curr Opin Struct Biol 2014;28:122–30. https://doi.org/10.1016/j.sbi.2014.08.005.
[78] Rosenbaum DM, Cherezov V, Hanson MA, Rasmussen SG, Thian FS, Kobilka TS, Choi HJ, Yao XJ, Weis WI, Stevens RC, Kobilka BK. GPCR engineering yields high-resolution structural insights into beta2-adrenergic receptor function. Science 2007;318:1266–73. https://doi.org/10.1126/science.1150609.
[79] Wu B, Chien EYT, Mol CD, Fenalti G, Liu W, Katritch V, Abagyan R, Brooun A, Wells P, Bi FC, Hamel DJ, Kuhn P, Handel TM, Cherezov V, Stevens RC. Structures of the CXCR4 chemokine GPCR with small-molecule and cyclic peptide antagonists. Science (New York, NY) 2010;330:1066–71. https://doi.org/10.1126/science.1194396.
[80] Shimamura T, Shiroishi M, Weyand S, Tsujimoto H, Winter G, Katritch V, Abagyan R, Cherezov V, Liu W, Han GW, Kobayashi T, Stevens RC, Iwata S. Structure of the human histamine H1 receptor complex with doxepin. Nature 2011;475:65–70. https://doi.org/10.1038/nature10236.

[81] Chien EYT, Liu W, Zhao Q, Katritch V, Won Han G, Hanson MA, Shi L, Newman AH, Javitch JA, Cherezov V, Stevens RC. Structure of the human dopamine D3 receptor in complex with a D2/D3 selective antagonist. Science 2010;330:1091–5. https://doi.org/10.1126/science.1197410.

[82] Rosenbaum DM, Rasmussen SGF, Kobilka BK. The structure and function of G-protein-coupled receptors. Nature 2009;459:356–63. https://doi.org/10.1038/nature08144.

[83] Landry JP, Ke Y, Yu G-L, Zhu XD. Measuring affinity constants of 1450 monoclonal antibodies to peptide targets with a microarray-based label-free assay platform. J Immunol Methods 2015;417:86–96. https://doi.org/10.1016/j.jim.2014.12.011.

[84] Iwata S, Ostermeier C, Ludwig B, Michel H. Structure at 2.8 Å resolution of cytochrome c oxidase from *Paracoccus denitrificans*. Nature 1995;376:660–9. https://doi.org/10.1038/376660a0.

[85] Zhou Y, Morais-Cabral JH, Kaufman A, MacKinnon R. Chemistry of ion coordination and hydration revealed by a K + channel-Fab complex at 2.0 Å resolution. Nature 2001;414:43–8. https://doi.org/10.1038/35102009.

[86] Dutzler R, Campbell EB, Cadene M, Chait BT, MacKinnon R. X-ray structure of a ClC chloride channel at 3.0 Å reveals the molecular basis of anion selectivity. Nature 2002;415:287–94. https://doi.org/10.1038/415287a.

[87] Hino T, Matsumoto Y, Nagano S, Sugimoto H, Fukumori Y, Murata T, Iwata S, Shiro Y. Structural basis of biological N_2O generation by bacterial nitric oxide reductase. Science 2010;330:1666–70. https://doi.org/10.1126/science.1195591.

[88] Tsukazaki T, Mori H, Fukai S, Ishitani R, Mori T, Dohmae N, Perederina A, Sugita Y, Vassylyev DG, Ito K, Nureki O. Conformational transition of Sec machinery inferred from bacterial SecYE structures. Nature 2008;455:988–91. https://doi.org/10.1038/nature07421.

[89] Ghosh E, Kumari P, Jaiman D, Shukla AK. Methodological advances: the unsung heroes of the GPCR structural revolution. Nat Rev Mol Cell Biol 2015;16:69–81. https://doi.org/10.1038/nrm3933.

[90] McMahon C, Baier AS, Pascolutti R, Wegrecki M, Zheng S, Ong JX, Erlandson SC, Hilger D, Rasmussen SGF, Ring AM, Manglik A, Kruse AC. Yeast surface display platform for rapid discovery of conformationally selective nanobodies. Nat Struct Mol Biol 2018;25:289–96. https://doi.org/10.1038/s41594-018-0028-6.

[91] Pardon E, Laeremans T, Triest S, Rasmussen SGF, Wohlkönig A, Ruf A, Muyldermans S, Hol WGJ, Kobilka BK, Steyaert J. A general protocol for the generation of nanobodies for structural biology. Nat Protoc 2014;9:674–93. https://doi.org/10.1038/nprot.2014.039.

[92] Uchański T, Zögg T, Yin J, Yuan D, Wohlkönig A, Fischer B, Rosenbaum DM, Kobilka BK, Pardon E, Steyaert J. An improved yeast surface display platform for the screening of nanobody immune libraries. Sci Rep 2019;9:382. https://doi.org/10.1038/s41598-018-37212-3.

[93] Zimmermann I, Egloff P, Hutter CAJ, Arnold FM, Stohler P, Bocquet N, Hug MN, Huber S, Siegrist M, Hetemann L, Gera J, Gmür S, Spies P, Gygax D, Geertsma ER, Dawson RJP, Seeger MA. Synthetic single domain antibodies for the conformational trapping of membrane proteins. Elife 2018;7, e34317. https://doi.org/10.7554/eLife.34317.

[94] Wingler LM, McMahon C, Staus DP, Lefkowitz RJ, Kruse AC. Distinctive activation mechanism for angiotensin receptor revealed by a synthetic nanobody. Cell 2019;176. https://doi.org/10.1016/j.cell.2018.12.006. 479-490.e412.

[95] Bräuer P, Parker JL, Gerondopoulos A, Zimmermann I, Seeger MA, Barr FA, Newstead S. Structural basis for pH-dependent retrieval of ER proteins from the Golgi by the KDEL receptor. Science 2019;363:1103. https://doi.org/10.1126/science.aaw2859.

[96] Hutter CAJ, Timachi MH, Hürlimann LM, Zimmermann I, Egloff P, Göddeke H, Kucher S, Štefanić S, Karttunen M, Schäfer LV, Bordignon E, Seeger MA. The extracellular gate shapes the energy profile of an ABC exporter. Nat Commun 2019;10:2260. https://doi.org/10.1038/s41467-019-09892-6.
[97] Arnold FM, Weber MS, Gonda I, Gallenito MJ, Adenau S, Egloff P, Zimmermann I, Hutter CAJ, Hürlimann LM, Peters EE, Piel J, Meloni G, Medalia O, Seeger MA. The ABC exporter IrtAB imports and reduces mycobacterial siderophores. Nature 2020;580:413–7. https://doi.org/10.1038/s41586-020-2136-9.
[98] Walter JD, Hutter CAJ, Zimmermann I, Earp J, Egloff P, Sorgenfrei M, Hürlimann LM, Gonda I, Meier G, Remm S, Thavarasah S, Plattet P, Seeger MA. Synthetic nanobodies targeting the SARS-CoV-2 receptor-binding domain. bioRxiv 2020. https://doi.org/10.1101/2020.04.16.045419.
[99] Koide A, Bailey CW, Huang X, Koide S. The fibronectin type III domain as a scaffold for novel binding proteins 11 edited by J. Wells. J Mol Biol 1998;284:1141–51. https://doi.org/10.1006/jmbi.1998.2238.
[100] Karatan E, Merguerian M, Han Z, Scholle MD, Koide S, Kay BK. Molecular recognition properties of FN3 monobodies that bind the Src SH3 domain. Chem Biol 2004;11:835–44. https://doi.org/10.1016/j.chembiol.2004.04.009.
[101] Koide A, Wojcik J, Gilbreth RN, Hoey RJ, Koide S. Teaching an old scaffold new tricks: monobodies constructed using alternative surfaces of the FN3 scaffold. J Mol Biol 2012;415:393–405. https://doi.org/10.1016/j.jmb.2011.12.019.
[102] Kermani AA, Burata OE, Koff BB, Koide A, Koide S, Stockbridge RB. Crystal structures of bacterial small multidrug resistance transporter EmrE in complex with structurally diverse substrates. eLife 2022;11:e76766. https://doi.org/10.7554/eLife.76766.
[103] Sha F, Salzman G, Gupta A, Koide S. Monobodies and other synthetic binding proteins for expanding protein science. Protein Sci 2017;26:910–24. https://doi.org/10.1002/pro.3148.
[104] Stockbridge RB, Kolmakova-Partensky L, Shane T, Koide A, Koide S, Miller C, Newstead S. Crystal structures of a double-barrelled fluoride ion channel. Nature 2015;525:548–51. https://doi.org/10.1038/nature14981.
[105] Koide A, Gilbreth RN, Esaki K, Tereshko V, Koide S. High-affinity single-domain binding proteins with a binary-code interface. Proc Natl Acad Sci U S A 2007;104:6632–7. https://doi.org/10.1073/pnas.0700149104.
[106] Gushchin I, Melnikov I, Polovinkin V, Ishchenko A, Yuzhakova A, Buslaev P, Bourenkov G, Grudinin S, Round E, Balandin T, Borshchevskiy V, Willbold D, Leonard G, Buldt G, Popov A, Gordeliy V. Mechanism of transmembrane signaling by sensor histidine kinases. Science 2017;356. https://doi.org/10.1126/science.aah6345.
[107] Gushchin I, Melnikov I, Polovinkin V, Ishchenko A, Gordeliy V. Crystal structure of a proteolytic fragment of the sensor histidine kinase NarQ. Crystals 2020;10. https://doi.org/10.3390/cryst10030149.
[108] Deller MC, Kong L, Rupp B. Protein stability: a crystallographer's perspective. Acta Crystallogr F Struct Biol Commun 2016;72:72–95. https://doi.org/10.1107/S2053230X15024619.
[109] Chung IYW, Li L, Tyurin O, Gagarinova A, Wibawa R, Li P, Hartland EL, Cygler M. Structural and functional study of Legionella pneumophila effector RavA. Protein Sci 2021;30:940–55. https://doi.org/10.1002/pro.4057.
[110] Zhang Y, Prach LM, O'Brien TE, DiMaio F, Prigozhin DM, Corn JE, Alber T, Siegel JB, Tantillo DJ. Crystal structure and mechanistic molecular modeling studies of *Mycobacterium tuberculosis* diterpene cyclase Rv3377c. Biochemistry 2020;59:4507–15. https://doi.org/10.1021/acs.biochem.0c00762.

[111] Andaleeb H, Ullah N, Falke S, Perbandt M, Brognaro H, Betzel C. High-resolution crystal structure and biochemical characterization of a GH11 endoxylanase from *Nectria haematococca*. Sci Rep 2020;10:15658. https://doi.org/10.1038/s41598-020-72644-w.
[112] Sato Y, Tsuchiya H, Yamagata A, Okatsu K, Tanaka K, Saeki Y, Fukai S. Structural insights into ubiquitin recognition and Ufd1 interaction of Npl4. Nat Commun 2019;10:5708. https://doi.org/10.1038/s41467-019-13697-y.
[113] Kung WW, Ramachandran S, Makukhin N, Bruno E, Ciulli A. Structural insights into substrate recognition by the SOCS2 E3 ubiquitin ligase. Nat Commun 2019;10:2534. https://doi.org/10.1038/s41467-019-10190-4.
[114] Cooper DR, Boczek T, Grelewska K, Pinkowska M, Sikorska M, Zawadzki M, Derewenda Z. Protein crystallization by surface entropy reduction: optimization of the SER strategy. Acta Crystallogr D Biol Crystallogr 2007;63:636–45. https://doi.org/10.1107/s0907444907010931.
[115] Goldschmidt L, Cooper DR, Derewenda ZS, Eisenberg D. Toward rational protein crystallization: a web server for the design of crystallizable protein variants. Protein Sci 2007;16:1569–76. https://doi.org/10.1110/ps.072914007.
[116] Vaidehi N, Grisshammer R, Tate CG. How can mutations thermostabilize G-protein-coupled receptors? Trends Pharmacol Sci 2016;37:37–46. https://doi.org/10.1016/j.tips.2015.09.005.
[117] Christopher JA, Brown J, Doré AS, Errey JC, Koglin M, Marshall FH, Myszka DG, Rich RL, Tate CG, Tehan B, Warne T, Congreve M. Biophysical fragment screening of the β1-adrenergic receptor: identification of high affinity arylpiperazine leads using structure-based drug design. J Med Chem 2013;56:3446–55. https://doi.org/10.1021/jm400140q.
[118] Warne T, Edwards PC, Leslie AG, Tate CG. Crystal structures of a stabilized β1-adrenoceptor bound to the biased agonists bucindolol and carvedilol. Structure 2012;20:841–9. https://doi.org/10.1016/j.str.2012.03.014.
[119] Warne T, Moukhametzianov R, Baker JG, Nehmé R, Edwards PC, Leslie AGW, Schertler GFX, Tate CG. The structural basis for agonist and partial agonist action on a β(1)-adrenergic receptor. Nature 2011;469:241–4. https://doi.org/10.1038/nature09746.
[120] Warne T, Serrano-Vega MJ, Baker JG, Moukhametzianov R, Edwards PC, Henderson R, Leslie AG, Tate CG, Schertler GF. Structure of a beta1-adrenergic G-protein-coupled receptor. Nature 2008;454:486–91. https://doi.org/10.1038/nature07101.
[121] Robertson N, Jazayeri A, Errey J, Baig A, Hurrell E, Zhukov A, Langmead CJ, Weir M, Marshall FH. The properties of thermostabilised G protein-coupled receptors (StaRs) and their use in drug discovery. Neuropharmacology 2011;60:36–44. https://doi.org/10.1016/j.neuropharm.2010.07.001.
[122] Lebon G, Warne T, Edwards PC, Bennett K, Langmead CJ, Leslie AG, Tate CG. Agonist-bound adenosine A2A receptor structures reveal common features of GPCR activation. Nature 2011;474:521–5. https://doi.org/10.1038/nature10136.
[123] Krumm BE, White JF, Shah P, Grisshammer R. Structural prerequisites for G-protein activation by the neurotensin receptor. Nat Commun 2015;6:7895. https://doi.org/10.1038/ncomms8895.
[124] Tan Q, Zhu Y, Li J, Chen Z, Han GW, Kufareva I, Li T, Ma L, Fenalti G, Li J, Zhang W, Xie X, Yang H, Jiang H, Cherezov V, Liu H, Stevens RC, Zhao Q, Wu B. Structure of the CCR5 chemokine receptor-HIV entry inhibitor maraviroc complex. Science (New York, NY) 2013;341:1387–90. https://doi.org/10.1126/science.1241475.
[125] Srivastava A, Yano J, Hirozane Y, Kefala G, Gruswitz F, Snell G, Lane W, Ivetac A, Aertgeerts K, Nguyen J, Jennings A, Okada K. High-resolution structure of the

human GPR40 receptor bound to allosteric agonist TAK-875. Nature 2014; 513:124–7. https://doi.org/10.1038/nature13494.
[126] Hollenstein K, Kean J, Bortolato A, Cheng RK, Doré AS, Jazayeri A, Cooke RM, Weir M, Marshall FH. Structure of class B GPCR corticotropin-releasing factor receptor 1. Nature 2013;499:438–43. https://doi.org/10.1038/nature12357.
[127] Doré AS, Okrasa K, Patel JC, Serrano-Vega M, Bennett K, Cooke RM, Errey JC, Jazayeri A, Khan S, Tehan B, Weir M, Wiggin GR, Marshall FH. Structure of class C GPCR metabotropic glutamate receptor 5 transmembrane domain. Nature 2014;511:557–62. https://doi.org/10.1038/nature13396.
[128] Munk C, Mutt E, Isberg V, Nikolajsen LF, Bibbe JM, Flock T, Hanson MA, Stevens RC, Deupi X, Gloriam DE. An online resource for GPCR structure determination and analysis. Nat Methods 2019;16:151–62. https://doi.org/10.1038/s41592-018-0302-x.
[129] Penmatsa A, Wang KH, Gouaux E. X-ray structure of dopamine transporter elucidates antidepressant mechanism. Nature 2013;503:85–90. https://doi.org/10.1038/nature12533.
[130] Chen L, Dürr KL, Gouaux E. X-ray structures of AMPA receptor-cone snail toxin complexes illuminate activation mechanism. Science 2014;345:1021–6. https://doi.org/10.1126/science.1258409.
[131] Debruycker V, Hutchin A, Masureel M, Ficici E, Martens C, Legrand P, Stein RA, McHaourab HS, Faraldo-Gómez JD, Remaut H, Govaerts C. An embedded lipid in the multidrug transporter LmrP suggests a mechanism for polyspecificity. Nat Struct Mol Biol 2020;27:829–35. https://doi.org/10.1038/s41594-020-0464-y.
[132] Raynal B, Lenormand P, Baron B, Hoos S, England P. Quality assessment and optimization of purified protein samples: why and how? Microb Cell Factories 2014;13:180. https://doi.org/10.1186/s12934-014-0180-6.
[133] Pignataro MF, Herrera MG, Dodero VI. Evaluation of peptide/protein self-assembly and aggregation by spectroscopic methods. Molecules 2020;25:4854. https://doi.org/10.3390/molecules25204854.
[134] McMullan D, Canaves JM, Quijano K, Abdubek P, Nigoghossian E, Haugen J, Klock HE, Vincent J, Hale J, Paulsen J, Lesley SA. High-throughput protein production for X-ray crystallography and use of size exclusion chromatography to validate or refute computational biological unit predictions. J Struct Funct Genom 2005;6:135–41. https://doi.org/10.1007/s10969-005-2898-1.
[135] Wilson WW. Monitoring crystallization experiments using dynamic light scattering: assaying and monitoring protein crystallization in solution. Methods 1990;1:110–7. https://doi.org/10.1016/S1046-2023(05)80154-9.
[136] Al-Ghobashy MA, Mostafa MM, Abed HS, Fathalla FA, Salem MY. Correlation between dynamic light scattering and size exclusion high performance liquid chromatography for monitoring the effect of pH on stability of biopharmaceuticals. J Chromatogr B Anal Technol Biomed Life Sci 2017;1060:1–9. https://doi.org/10.1016/j.jchromb.2017.05.029.
[137] Some D, Amartely H, Tsadok A, Lebendiker M. Characterization of proteins by size-exclusion chromatography coupled to multi-angle light scattering (SEC-MALS). J Vis Exp 2019;, e59615. https://doi.org/10.3791/59615.
[138] Russo Krauss I, Merlino A, Vergara A, Sica F. An overview of biological macromolecule crystallization. Int J Mol Sci 2013;14:11643–91. https://doi.org/10.3390/ijms140611643.
[139] Hiraki M, Kato R, Nagai M, Satoh T, Hirano S, Ihara K, Kudo N, Nagae M, Kobayashi M, Inoue M. Development of an automated large-scale protein-crystallization and monitoring system for high-throughput protein-structure analyses. Acta Crystallogr D Biol Crystallogr 2006;62:1058–65.

[140] Sugahara M, Asada Y, Shimizu K, Yamamoto H, Lokanath NK, Mizutani H, Bagautdinov B, Matsuura Y, Taketa M, Kageyama Y. High-throughput crystallization-to-structure pipeline at RIKEN SPring-8 Center. J Struct Funct Genom 2008;9:21–8.
[141] Gorrec F, Löwe J. Automated protocols for macromolecular crystallization at the MRC laboratory of molecular biology. J Vis Exp 2018.
[142] Shaw Stewart P, Mueller-Dieckmann J. Automation in biological crystallization. Acta Crystallogr F: Struct Biol Commun 2014;70:686–96.
[143] Bard J, Ercolani K, Svenson K, Olland A, Somers W. Automated systems for protein crystallization. Methods 2004;34:329–47.
[144] Shah AK, Liu Z-J, Stewart PD, Schubot FD, Rose JP, Newton MG, Wang B-C. On increasing protein-crystallization throughput for X-ray diffraction studies. Acta Crystallogr D Biol Crystallogr 2005;61:123–9.
[145] Landau EM, Rosenbusch JP. Lipidic cubic phases: a novel concept for the crystallization of membrane proteins. Proc Natl Acad Sci 1996;93:14532–5.
[146] Salvati Manni L, Zabara A, Osornio YM, Schöppe J, Batyuk A, Plückthun A, Siegel JS, Mezzenga R, Landau EM. Phase behavior of a designed cyclopropyl analogue of monoolein: implications for low-temperature membrane protein crystallization. Angew Chem Int Ed 2015;54:1027–31.
[147] Borshchevskiy V, Moiseeva E, Kuklin A, Büldt G, Hato M, Gordeliy V. Isoprenoid-chained lipid β-XylOC16 + 4—a novel molecule for in meso membrane protein crystallization. J Cryst Growth 2010;312:3326–30.
[148] Misquitta LV, Misquitta Y, Cherezov V, Slattery O, Mohan JM, Hart D, Zhalnina M, Cramer WA, Caffrey M. Membrane protein crystallization in lipidic mesophases with tailored bilayers. Structure 2004;12:2113–24.
[149] Ishchenko A, Peng L, Zinovev E, Vlasov A, Lee SC, Kuklin A, Mishin A, Borshchevskiy V, Zhang Q, Cherezov V. Chemically stable lipids for membrane protein crystallization. Cryst Growth Des 2017;17:3502–11.
[150] Kato R, Hiraki M, Yamada Y, Tanabe M, Senda T. A fully automated crystallization apparatus for small protein quantities. Acta Crystallogr F: Struct Biol Commun 2021;77.
[151] Perry SL, Guha S, Pawate AS, Bhaskarla A, Agarwal V, Nair SK, Kenis PJ. A microfluidic approach for protein structure determination at room temperature via on-chip anomalous diffraction. Lab Chip 2013;13:3183–7.
[152] Junius N, Oksanen E, Terrien M, Berzin C, Ferrer J-L, Budayova-Spano M. A crystallization apparatus for temperature-controlled flow-cell dialysis with real-time visualization. J Appl Crystallogr 2016;49:806–13.
[153] Laval P, Giroux C, Leng J, Salmon J-B. Microfluidic screening of potassium nitrate polymorphism. J Cryst Growth 2008;310:3121–4.
[154] Dhouib K, Malek CK, Pfleging W, Gauthier-Manuel B, Duffait R, Thuillier G, Ferrigno R, Jacquamet L, Ohana J, Ferrer J-L. Microfluidic chips for the crystallization of biomacromolecules by counter-diffusion and on-chip crystal X-ray analysis. Lab Chip 2009;9:1412–21.
[155] Hansen CL, Skordalakes E, Berger JM, Quake SR. A robust and scalable microfluidic metering method that allows protein crystal growth by free interface diffusion. Proc Natl Acad Sci 2002;99:16531–6.
[156] Talreja S, Kim DY, Mirarefi AY, Zukoski CF, Kenis PJ. Screening and optimization of protein crystallization conditions through gradual evaporation using a novel crystallization platform. J Appl Crystallogr 2005;38:988–95.
[157] Li L, Mustafi D, Fu Q, Tereshko V, Chen DL, Tice JD, Ismagilov RF. Nanoliter microfluidic hybrid method for simultaneous screening and optimization validated with crystallization of membrane proteins. Proc Natl Acad Sci 2006;103:19243–8.
[158] Du W, Li L, Nichols KP, Ismagilov RF. SlipChip. Lab Chip 2009;9:2286–92.

[159] Li L, Ismagilov RF. Protein crystallization using microfluidic technologies based on valves, droplets, and SlipChip. Annu Rev Biophys 2010;39:139–58.
[160] Lau BT, Baitz CA, Dong XP, Hansen CL. A complete microfluidic screening platform for rational protein crystallization. J Am Chem Soc 2007;129:454–5.
[161] Zheng B, Gerdts CJ, Ismagilov RF. Using nanoliter plugs in microfluidics to facilitate and understand protein crystallization. Curr Opin Struct Biol 2005;15:548–55.
[162] Hansen CL, Sommer MO, Quake SR. Systematic investigation of protein phase behavior with a microfluidic formulator. Proc Natl Acad Sci 2004;101:14431–6.
[163] Skou M, Skou S, Jensen TG, Vestergaard B, Gillilan RE. In situ microfluidic dialysis for biological small-angle X-ray scattering. J Appl Crystallogr 2014;47:1355–66.
[164] Scrimgeour J, Cho JK, Breedveld V, Curtis J. Microfluidic dialysis cell for characterization of macromolecule interactions. Soft Matter 2011;7:4762–7.
[165] Junius N, Jaho S, Sallaz-Damaz Y, Borel F, Salmon J-B, Budayova-Spano M. A microfluidic device for both on-chip dialysis protein crystallization and in situ X-ray diffraction. Lab Chip 2020;20:296–310.
[166] Li Y, Xuan J, Hu R, Zhang P, Lou X, Yang Y. Microfluidic triple-gradient generator for efficient screening of chemical space. Talanta 2019;204:569–75.
[167] Sui S, Mulichak A, Kulathila R, Mcgee J, Filiatreault D, Saha S, Cohen A, Song J, Hung H, Selway J, Kirby C, Shrestha OK, Weihofen W, Fodor M, Xu M, Chopra R, Perry SL. A capillary-based microfluidic device enables primary high-throughput room-temperature crystallographic screening. J Appl Crystallogr 2021;54:1034–46. https://doi.org/10.1107/s1600576721004155.
[168] Heymann M, Opthalage A, Wierman JL, Akella S, Szebenyi DM, Gruner SM, Fraden S. Room-temperature serial crystallography using a kinetically optimized microfluidic device for protein crystallization and on-chip X-ray diffraction. IUCrJ 2014;1:349–60.
[169] Gicquel Y, Schubert R, Kapis S, Bourenkov G, Schneider T, Perbandt M, Betzel C, Chapman HN, Heymann M. Microfluidic chips for in situ crystal X-ray diffraction and in situ dynamic light scattering for serial crystallography. J Vis Exp 2018.
[170] Perry SL, Guha S, Pawate AS, Henning R, Kosheleva I, Srajer V, Kenis PJ, Ren Z. In situ serial Laue diffraction on a microfluidic crystallization device. J Appl Crystallogr 2014;47:1975–82.
[171] Pinker F, Brun M, Morin P, Deman A-L, Chateaux J-FO, Oliéric V, Stirnimann C, Lorber B, Terrier N, Ferrigno R. ChipX: a novel microfluidic chip for counter-diffusion crystallization of biomolecules and in situ crystal analysis at room temperature. Cryst Growth Des 2013;13:3333–40.
[172] Sui S, Wang Y, Dimitrakopoulos C, Perry SL. A graphene-based microfluidic platform for electrocrystallization and in situ X-ray diffraction. Crystals 2018;8:76.
[173] Maeki M, Pawate AS, Yamashita K, Kawamoto M, Tokeshi M, Kenis PJ, Miyazaki M. A method of cryoprotection for protein crystallography by using a microfluidic chip and its application for in situ X-ray diffraction measurements. Anal Chem 2015;87:4194–200.
[174] Sommer MO, Larsen S. Crystallizing proteins on the basis of their precipitation diagram determined using a microfluidic formulator. J Synchrotron Radiat 2005;12:779–85.
[175] Li L, Fu Q, Kors CA, Stewart L, Nollert P, Laible PD, Ismagilov RF. A plug-based microfluidic system for dispensing lipidic cubic phase (LCP) material validated by crystallizing membrane proteins in lipidic mesophases. Microfluid Nanofluid 2010;8:789–98.
[176] Perry SL, Roberts GW, Tice JD, Gennis RB, Kenis PJ. Microfluidic generation of lipidic mesophases for membrane protein crystallization. Cryst Growth Des 2009;9:2566–9.
[177] Pinker F, Brun M, Morin P, Deman A-L, Chateaux J-F, Oliéric V, Stirnimann C, Lorber B, Terrier N, Ferrigno R, Sauter C. ChipX: a novel microfluidic chip for counter-diffusion crystallization of biomolecules and in situ crystal analysis at room temperature. Cryst Growth Des 2013;13:3333–40. https://doi.org/10.1021/cg301757g.

[178] Garman EF. Radiation damage in macromolecular crystallography: what is it and why should we care? Acta Crystallogr D Biol Crystallogr 2010;66:339–51.
[179] Zhou R-B, Cao H-L, Zhang C-Y, Yin D-C. A review on recent advances for nucleants and nucleation in protein crystallization. CrystEngComm 2017;19:1143–55. https://doi.org/10.1039/c6ce02562e.
[180] Saridakis E, Chayen NE. Towards a 'universal' nucleant for protein crystallization. Trends Biotechnol 2009;27:99–106.
[181] Nanev CN, Saridakis E, Chayen NE. Protein crystal nucleation in pores. Sci Rep 2017;7:35821. https://doi.org/10.1038/srep35821.
[182] Khurshid S, Saridakis E, Govada L, Chayen NE. Porous nucleating agents for protein crystallization. Nat Protoc 2014;9:1621–33.
[183] Shah UV, Williams DR, Heng JY. Selective crystallization of proteins using engineered nanonucleants. Cryst Growth Des 2012;12:1362–9.
[184] Guo Y-Z, Sun L-H, Oberthuer D, Zhang C-Y, Shi J-Y, Di J-L, Zhang B-L, Cao H-L, Liu Y-M, Li J. Utilisation of adsorption and desorption for simultaneously improving protein crystallisation success rate and crystal quality. Sci Rep 2014;4:1–8.
[185] Zhou T, Zhang K, Kamra T, Bülow L, Ye L. Preparation of protein imprinted polymer beads by pickering emulsion polymerization. J Mater Chem B 2015;3:1254–60.
[186] Vasapollo G, Sole RD, Mergola L, Lazzoi MR, Scardino A, Scorrano S, Mele G. Molecularly imprinted polymers: present and future prospective. Int J Mol Sci 2011;12:5908–45.
[187] Saridakis E, Khurshid S, Govada L, Phan Q, Hawkins D, Crichlow GV, Lolis E, Reddy SM, Chayen NE. Protein crystallization facilitated by molecularly imprinted polymers. Proc Natl Acad Sci 2011;108:11081–6.
[188] Saridakis E, Chayen NE. Imprinted polymers assisting protein crystallization. Trends Biotechnol 2013;31:515–20.
[189] Khurshid S, Govada L, El-Sharif HF, Reddy SM, Chayen NE. Automating the application of smart materials for protein crystallization. Acta Crystallogr D Biol Crystallogr 2015;71:534–40.
[190] Xing Y, Hu Y, Jiang L, Gao Z, Chen Z, Chen Z, Ren X. Zwitterion-immobilized imprinted polymers for promoting the crystallization of proteins. Cryst Growth Des 2015;15:4932–7.
[191] Clares MP, Serena C, Blasco S, Nebot A, del Castillo L, Soriano C, Domènech A, Sánchez-Sánchez AV, Soler-Calero L, Mullor JL. Mn (II) complexes of scorpiand-like ligands. A model for the MnSOD active centre with high in vitro and in vivo activity. J Inorg Biochem 2015;143:1–8.
[192] Weis WI, Kahn R, Fourme R, Drickamer K, Hendrickson WA. Structure of the calcium-dependent lectin domain from a rat mannose-binding protein determined by MAD phasing. Science 1991;254:1608–15.
[193] Silvaggi NR, Martin LJ, Schwalbe H, Imperiali B, Allen KN. Double-lanthanide-binding tags for macromolecular crystallographic structure determination. J Am Chem Soc 2007;129:7114–20.
[194] Girard É, Stelter M, Vicat J, Kahn R. A new class of lanthanide complexes to obtain high-phasing-power heavy-atom derivatives for macromolecular crystallography. Acta Crystallogr D Biol Crystallogr 2003;59:1914–22.
[195] Pompidor G, d'Aleo A, Vicat J, Toupet L, Giraud N, Kahn R, Maury O. Protein crystallography through supramolecular interactions between a lanthanide complex and arginine. Angew Chem 2008;120:3436–9.
[196] Stelter M, Molina R, Jeudy S, Kahn R, Abergel C, Hermoso JA. A complement to the modern crystallographer's toolbox: caged gadolinium complexes with versatile binding modes. Acta Crystallogr D Biol Crystallogr 2014;70:1506–16.
[197] Engilberge S, Riobé F, Di Pietro S, Lassalle L, Coquelle N, Arnaud C-A, Pitrat D, Mulatier J-C, Madern D, Breyton C. Crystallophore: a versatile lanthanide complex

for protein crystallography combining nucleating effects, phasing properties, and luminescence. Chem Sci 2017;8:5909–17.
[198] Kumari Yadav R, Krishnan V. The adhesive PitA pilus protein from the early dental plaque colonizer *Streptococcus oralis*: expression, purification, crystallization and X-ray diffraction analysis. Acta Crystallogr F: Struct Biol Commun 2020;76:8–13.
[199] Prieto-Castañeda A, Martínez-Caballero S, Agarrabeitia AR, García-Moreno I, Moya SDL, Ortiz MJ, Hermoso JA. First lanthanide complex for de novo phasing in native protein crystallography at 1 Å radiation. ACS Appl Bio Mater 2021;4:4575–81. https://doi.org/10.1021/acsabm.1c00305.
[200] McPherson A, Shlichta P. Heterogeneous and epitaxial nucleation of protein crystals on mineral surfaces. Science 1988;239:385–7. https://doi.org/10.1126/science.239.4838.385.
[201] Akella SV, Mowitz A, Heymann M, Fraden S. Emulsion-based technique to measure protein crystal nucleation rates of lysozyme. Cryst Growth Des 2014;14:4487–509. https://doi.org/10.1021/cg500562r.
[202] Chayen NE, Saridakis E, El Bahar R, Nemirovsky Y. Porous silicon: a nucleation-inducing material for protein crystallization. Acta Crystallogr Sect A: Found Crystallogr 2002;58:c224. https://doi.org/10.1107/s0108767302093972.
[203] Stewart PS, Mueller-Dieckmann J. Automation in biological crystallization. Acta Crystallogr F Struct Biol Commun 2014;70:686–96. https://doi.org/10.1107/s2053230x14011601.
[204] Zhu Y, Zhu L-N, Guo R, Cui H-J, Ye S, Fang Q. Nanoliter-scale protein crystallization and screening with a microfluidic droplet robot. Sci Rep 2014;4:5046. https://doi.org/10.1038/srep05046.
[205] Dauter Z, Wlodawer A. Progress in protein crystallography. Protein Pept Lett 2016;23:201–10. https://doi.org/10.2174/0929866523666160106153524.
[206] Desbois S, Seabrook SA, Newman J. Some practical guidelines for UV imaging in the protein crystallization laboratory. Acta Crystallogr Sect F: Struct Biol Cryst Commun 2013;69:201–8. https://doi.org/10.1107/S1744309112048634.
[207] Weber P, Pissis C, Navaza R, Mechaly AE, Saul F, Alzari PM, Haouz A. High-throughput crystallization pipeline at the crystallography core facility of the Institut Pasteur. Molecules 2019;24:4451.
[208] Owen RL, Juanhuix J, Fuchs M. Current advances in synchrotron radiation instrumentation for MX experiments. Arch Biochem Biophys 2016;602:21–31. https://doi.org/10.1016/j.abb.2016.03.021.
[209] Yamamoto M, Hirata K, Yamashita K, Hasegawa K, Ueno G, Ago H, Kumasaka T. Protein microcrystallography using synchrotron radiation. IUCrJ 2017;4:5 29–39. https://doi.org/10.1107/s2052252517008193.
[210] Duke EMH, Johnson LN. Macromolecular crystallography at synchrotron radiation sources: current status and future developments. Proc R Soc A: Math Phys Eng Sci 2010;466:3421–52. https://doi.org/10.1098/rspa.2010.0448.
[211] Cohen AE. A new era of synchrotron-enabled macromolecular crystallography. Nat Methods 2021;18:433–4. https://doi.org/10.1038/s41592-021-01146-y.
[212] Martiel I, Olieric V, Caffrey M, Wang M. Chapter 1: Practical approaches for in situ x-ray crystallography: from high-throughput screening to serial data collection. United Kingdom: Royal Society of Chemistry; 2018.
[213] Maveyraud L, Mourey L. Protein X-ray crystallography and drug discovery. Molecules 2020;25. https://doi.org/10.3390/molecules25051030.
[214] Broecker J, Morizumi T, Ou W-L, Klingel V, Kuo A, Kissick DJ, Ishchenko A, Lee M-Y, Xu S, Makarov O, Cherezov V, Ogata CM, Ernst OP. High-throughput in situ X-ray screening of and data collection from protein crystals at room temperature and under cryogenic conditions. Nat Protoc 2018;13:260–92. https://doi.org/10.1038/nprot.2017.135.

[215] Cipriani F, Röwer M, Landret C, Zander U, Felisaz F, Márquez JA. CrystalDirect: a new method for automated crystal harvesting based on laser-induced photoablation of thin films. Acta Crystallogr D Biol Crystallogr 2012;68:1393–9. https://doi.org/10.1107/s0907444912031459.
[216] Johansson LC, Stauch B, Ishchenko A, Cherezov V. A bright future for serial femtosecond crystallography with XFELs. Trends Biochem Sci 2017;42:749–62. https://doi.org/10.1016/j.tibs.2017.06.007.
[217] Liu H, Lee W. The XFEL protein crystallography: developments and perspectives. Int J Mol Sci 2019;20. https://doi.org/10.3390/ijms20143421.
[218] Martin-Garcia JM. Protein dynamics and time resolved protein crystallography at synchrotron radiation sources: past, present and future. Crystals 2021;11:521.
[219] Nogly P, Weinert T, James D, Carbajo S, Ozerov D, Furrer A, Gashi D, Borin V, Skopintsev P, Jaeger K, Nass K, Båth P, Bosman R, Koglin J, Seaberg M, Lane T, Kekilli D, Brünle S, Tanaka T, Wu W, Milne C, White T, Barty A, Weierstall U, Panneels V, Nango E, Iwata S, Hunter M, Schapiro I, Schertler G, Neutze R, Standfuss J. Retinal isomerization in bacteriorhodopsin captured by a femtosecond x-ray laser. Science 2018;361, eaat0094. https://doi.org/10.1126/science.aat0094.
[220] Jain D, Lamour V. Computational tools in protein crystallography. Methods Mol Biol 2010;673:129–56. https://doi.org/10.1007/978-1-60761-842-3_8.
[221] Powell HR. X-ray data processing. Biosci Rep 2017;37. https://doi.org/10.1042/bsr20170227.
[222] Adams PD, Afonine PV, Bunkóczi G, Chen VB, Davis IW, Echols N, Headd JJ, Hung LW, Kapral GJ, Grosse-Kunstleve RW, McCoy AJ, Moriarty NW, Oeffner R, Read RJ, Richardson DC, Richardson JS, Terwilliger TC, Zwart PH. PHENIX: a comprehensive Python-based system for macromolecular structure solution. Acta Crystallogr D Biol Crystallogr 2010;66:213–21. https://doi.org/10.1107/s0907444909052925.
[223] Pettersen EF, Goddard TD, Huang CC, Couch GS, Greenblatt DM, Meng EC, Ferrin TE. UCSF Chimera—a visualization system for exploratory research and analysis. J Comput Chem 2004;25:1605–12. https://doi.org/10.1002/jcc.20084.
[224] Aggarwal S, von Wachenfeldt C, Fisher SZ, Oksanen E. A protocol for production of perdeuterated OmpF porin for neutron crystallography. Protein Expr Purif 2021;188, 105954.